

ORIGINAL RESEARCH

Serine 26 in Early Growth Response-1 Is Critical for Endothelial Proliferation, Migration, and Network Formation

Fernando S. Santiago , PhD; Yue Li , MBBS, PhD; Levon M. Khachigian , PhD, DSc

BACKGROUND: Vascular endothelial cell proliferation, migration, and network formation are key proangiogenic processes involving the prototypic immediate early gene product, Egr-1 (early growth response-1). Egr-1 undergoes phosphorylation at a conserved Ser26 but its function is completely unknown in endothelial cells or any other cell type.

METHODS AND RESULTS: A CRISPR/Cas9 strategy was used to introduce a homozygous Ser26>Ala mutation into endogenous Egr-1 in human microvascular endothelial cells. In the course of generating mutant cells, we produced cells with homozygous deletion in *Egr-1* caused by frameshift and premature termination. We found that Ser26 mutation in Egr-1, or Egr-1 deletion, perturbed endothelial cell proliferation in models of cell counting or real-time growth using the xCELLigence System. We found that Ser26 mutation or Egr-1 deletion ameliorated endothelial cell migration toward VEGF-A₁₆₅ (vascular endothelial growth factor-A) in a dual-chamber model. On solubilized basement membrane preparations, Ser26 mutation or Egr-1 deletion prevented endothelial network (or tubule) formation, an in vitro model of angiogenesis. Flow cytometry further revealed that Ser26 mutation or Egr-1 deletion elevated early and late apoptosis. Finally, we demonstrated that Ser26 mutation or Egr-1 deletion increased VE-cadherin (vascular endothelial cadherin) expression, a regulator of endothelial adhesion and signaling, permeability, and angiogenesis.

CONCLUSIONS: These findings not only indicate that Egr-1 is essential for endothelial cell proliferation, migration, and network formation, but also show that point mutation in Ser26 is sufficient to impair each of these processes and trigger apoptosis as effectively as the absence of Egr-1. This highlights the importance of Ser26 in Egr-1 for a range of proangiogenic processes.

Key Words: CRISPR/Cas9 ■ early growth response-1 ■ endothelial cell ■ extracellular signal-regulated kinase-1

Egr-1 (early growth response-1) is the product of an immediate early gene also known as Krox24 and Tis8. It is a transcription factor that belongs to the Cys₂His₂ class of zinc finger proteins and typically recognizes the DNA binding motif, GCG(G/T)GGGCG.¹ When bound to DNA, Egr-1 can alter gene expression through mechanisms dependent on coactivators and corepressors. Egr-1 is typically poorly expressed in growth-quiescent cells but is rapidly and transiently expressed in response to extracellular agonists including growth factors and hormones,^{2–4} hypoxia,⁵ cytokines,^{2,6,7} shear stress,⁸ and a range of other agonists

and stresses.^{9–15} Egr-1 regulates several hundred genes in vascular endothelial cells, including genes controlling angiogenesis¹⁶ and a range of other biological processes.^{17–19} Our recent work in the international FANTOM5 (Functional Annotation of the Mammalian Genome 5) consortium revealed that *Egr-1* is among the most dynamic of all early response genes across a broad and diverse range of human cell types and stimuli.²⁰

The angiogenic process involves proliferation, migration, and network (also called tubule) formation by vascular endothelial cells and is regulated by factors

Correspondence to: Professor Levon Khachigian, PhD, DSc, MIP, Vascular Biology and Translational Research, School of Medical Sciences, UNSW Medicine and Health, University of New South Wales, Sydney, NSW 2052, Australia. E-mail: l.khachigian@unsw.edu.au

Supplementary Material for this article is available at <https://www.ahajournals.org/doi/suppl/10.1161/JAHA.120.020521>

For Sources of Funding and Disclosures, see page 13.

© 2021 The Authors. Published on behalf of the American Heart Association, Inc., by Wiley. This is an open access article under the terms of the Creative Commons Attribution-NonCommercial License, which permits use, distribution and reproduction in any medium, provided the original work is properly cited and is not used for commercial purposes.

JAHA is available at: www.ahajournals.org/journal/jaha

CLINICAL PERSPECTIVE

What Is New?

- We used a CRISPR/Cas9 strategy to introduce a homozygous Ser26>Ala mutation into endogenous Egr-1 in human vascular endothelial cells, and in the course of this exercise generated cells with homozygous deletion in *Egr-1* caused by frameshift and premature termination.
- Ser26 mutation in Egr-1, or Egr-1 deletion, perturbed serum-inducible endothelial cell proliferation, migration toward VEGF-A₁₆₅ (vascular endothelial growth factor-A), network (or tubule) formation on solubilized basement membrane preparations, elevated endothelial early and late apoptosis, and increased VE-cadherin (vascular endothelial cadherin) expression.
- Mutant and deletion cells had similar ability to proliferate, migrate, form networks, undergo apoptosis, and regulate VE-cadherin.

What Are the Clinical Implications?

- Our findings not only indicate that Egr-1 is essential for endothelial cell proliferation, migration, and network formation, but show that point mutation in Ser26 is sufficient to impair each of these endothelial processes and trigger apoptosis as effectively as the absence of Egr-1 itself.
- This underlines the potential importance of Ser26 in Egr-1 for a range of proangiogenic processes.

Nonstandard Abbreviations and Acronyms

CK2	casein kinase 2
EGF	epidermal growth factor
Egr-1	early growth response-1
ERK1	extracellular signal-regulated kinase-1
FBS	fetal bovine serum
FGF-2	fibroblast growth factor-2
HMEC-1	human microvascular endothelial cells
PDGF	platelet-derived growth factor
Ser26	serine residue in early growth response-1 at position 26
VE-cadherin	vascular endothelial cadherin
VEGF-A₁₆₅	vascular endothelial growth factor-A

such as VEGF-A₁₆₅ (vascular endothelial growth factor-A) and FGF-2 (fibroblast growth factor-2),²¹ which bind and activate receptors on the surface of endothelial

cells and initiate and promote the growth and survival of new blood vessels. Previously, we demonstrated that Egr-1 supports FGF-2-dependent angiogenesis in a murine model.² We also found that VEGF-A₁₆₅ stimulates FGF-2 expression in an Egr-1-dependent manner.² Egr-1 is controlled by ERK1 (extracellular signal-regulated kinase-1), which controls endothelial cell proliferation, migration, and angiogenesis.²²

Although it is well known that Egr-1 is phosphorylated,²³ we recently defined for the first time a specific amino acid in Egr-1 that undergoes phosphorylation. In vascular endothelial cells, the principal cells mediating angiogenesis, we discovered that ERK1 can phosphorylate a highly conserved serine residue in Egr-1 at position 26 (Ser26).²⁴ However, no study has yet identified a functional role for Ser26 nor any other phosphorylated residue in Egr-1 in any biological process. Understanding the importance of this residue in Egr-1 would provide important insights on how Egr-1-dependent gene-regulatory networks cross-communicate and function, and in turn, how this may impact biological processes including angiogenesis.

METHODS

The data that support the findings of this study are available from the corresponding author upon reasonable request.

Cell Culture

Human microvascular endothelial cells (HMEC-1) originally isolated from foreskin were obtained from the American Type Culture Collection (Rockville, MD) and grown in MCDB131 medium (Invitrogen, Waltham, MA) at pH 7.4 with 10% FBS, hydrocortisone (1 µg/mL), epidermal growth factor (10 ng/mL), L-glutamine (2 mmol/L), and penicillin/streptomycin (5 U/mL). Cells were routinely passaged with 0.05% trypsin/5 mmol/L EDTA and grown in a humidified atmosphere of 5% CO₂ at 37°C.

Generation of CRISPR/Cas9 HMEC-1 Cell Lines, Wild-Type, Mutant Ser26, and Deletion

CRISPR/Cas9 cell lines were generated with the approval of the University of New South Wales Gene Technology Research Committee. PX458 (pSpCas[BB]-2A-GFP) plasmid was a gift from Feng Zhang (Addgene plasmid no. 48138), and the protocol of CRISPR/Cas9 point mutation was adopted from Yik et al.²⁵ Five micrograms of PX458 was digested with *BbsI* (25 U) with New England Biolabs (Ipswich, MA) buffer 2.1 in a total volume of 40 µL, whereby digestion reaction was performed by incubating at 37°C for

1 hour. *BbsI* was heat inactivated at 65°C for 20 minutes before dephosphorylation by CIP (5 U) (New England Biolabs) at 37°C for 1 hour. Phosphatase was heat inactivated at 65°C for 20 minutes. Linearized and dephosphorylated plasmid was purified using Promega Wizard SV gel and polymerase chain reaction (PCR) Clean-Up System (Promega, Madison, WI).

Forward and reverse single-guide RNA oligonucleotides were designed following the design protocol from Ran et al.²⁶ Briefly, human *Egr-1* sequence (NM 001964.3) was loaded into a CRISPR/Cas9 single-guide RNA guide design platform (<http://crispr.mit.edu>), and guides were selected according to the score by reverse likelihood of off-target binding and if silent protospacer adjacent motif mutation could be obtained. Guide single-guide RNA oligonucleotides (forward 5'-**CAC CGA** GTG AGG AAA GGA TCC GAA C-3'; reverse 5'-**AAA** CGT TCG GAT CCT TTC CTC ACT C-3') (Sigma-Aldrich, St. Louis, MO) were phosphorylated separately with T4 polynucleotide kinase (New England Biolabs) before annealing. Extra nucleotides (in bold) were added to facilitate ligation into the PX458 plasmid. The annealed oligonucleotide was ligated into the PX458/*BbsI*/CIP-treated vector plasmid using the Quick T4 DNA ligase (New England Biolabs) and then transformed into XL-10 Gold ultracompetent cells (Agilent, Santa Clara, CA). Plasmids generated from transformants were screened by Sanger's capillary sequencing method.

HMEC-1 were transfected for 24 hours with PX458/human *Egr-1* guide and the donor *Egr-1m26* oligonucleotide (5'-ATG GCC GCG GCC AAG GCC GAG ATG CAG CTG ATG TCC CCG CTG CAG ATC TCT GAT CCG TTC GGA TCC TTT CCT CAC GCG CCC ACC ATG GAC AAC TAC CCT AAG CTG GAG GAG ATG ATG CTG CTG AGC AAC GGG GCT CCC CAG TTC CTC GGC-3') (Sigma-Aldrich) in the presence of lipofectamine (Invitrogen) and Opti-MEM medium (Invitrogen). CRISPR/Cas9 control cells were only transfected with pX458/human *Egr-1* plasmid without the donor oligonucleotide. Cells were sorted for GFP using BD FACS Aria II (BD Biosciences San Jose, CA) and green fluorescent protein-positive single cells were seeded into a 96-well plate containing HMEC-1 growth medium (MCDB 131; Invitrogen) supplemented with 10% FBS, 10 ng/mL epidermal growth factor (Sigma-Aldrich), 1 µg/mL hydrocortisone (Sigma-Aldrich), 2 mmol/L L-glutamine (Thermo Fisher Scientific, Waltham, MA), 5 U/mL penicillin–streptomycin (Thermo Fisher Scientific). Cells at almost 50% confluency were treated with Accutase (Thermo Fisher Scientific) to lift the cells and seeded into wells of a 6-well plate. At 80% confluency, the cells were seeded in triplicate in the 6-well plate. Cells from the 2 wells were frozen, whereas genomic DNA was extracted from cells in the third well.

Genomic DNA Extraction

Genomic DNA was extracted using the PureLink genomic kit (Invitrogen). Briefly, $\approx 5 \times 10^6$ CRISPR/Cas9 cell types were resuspended with 200 µL 1×PBS before addition of proteinase K and RNaseA. An equal volume (200 µL) of PureLink genomic lysis/binding buffer was added, mixed well, and incubated for 10 minutes at 55°C. Ethanol was added to the lysate and loaded into the spin columns. The columns were centrifuged at 10 000g for 1 minute at 22°C. The columns were washed as recommended with Wash Buffer 1 then with Wash Buffer 2 before DNA elution. Genomic DNA was eluted using sterile milliQ water and measured using a Nanodrop spectrophotometer. Aliquots of genomic DNA were stored at –20°C until further analysis.

CRISPR/Cas9 Screening

PCR-based screening of the CRISPR/Cas9/*Egr-1m26* and control was performed using 50 ng of genomic DNA with primers (*Egr-1* fwd139: 5'-CTG CAC GCT TCT CAG TGT TC-3' and *Egr-1* rvr565: 5'-AAA GAC TCT GCG GTC AGG TG-3') (Sigma-Aldrich). Amplification was done with Platinum SuperFi DNA polymerase (Thermo Fisher Scientific) with initial denaturation of 98°C for 30 seconds. Thirty-five cycles of 98°C for 10 seconds, 58°C for 10 seconds, and 72°C for 30 seconds were performed before further extension of 72°C for 5 minutes. The PCR reaction mixtures were submitted to the Ramaciotti Centre for Genomics (University of New South Wales) as core prep with EXOSAPIT clean-up before Sanger sequencing. Alternatively, the amplified 427 bp fragment was purified in 1.5% agarose gel in 1× Tris-acetate-EDTA buffer and further isolated using the Promega Wizard SV gel and PCR Clean-Up System (Promega). The purified PCR fragment was sequenced to confirm mutation of Ser26 to Ala26 (M26), control (wild-type) and *Egr-1* deletion cell types.

Copy Number Analysis

To test whether human *Egr-1* alleles had been homozygously modified in CRISPR/Cas9 mutant clones, quantitative PCR was done to calculate the copy number of *Egr-1* alleles. Quantitative PCR was performed using 10 ng of genomic DNA with 1× QuantiFast SYBR together with final concentration of 0.8 µmol/L primers in a total volume of 25 µL. Primers used were human *Egr-1*CFWD 5-ACT ACC CTA AGC TGG AGG AGA-3', human *Egr-1*CREV 5-GTG TCC GCC TGA GGG TTG A-3', human SP1F115 5'-AAT CGA GGA AGT GGA GGC AA-3', and human SP1R302 5-GGA GTC AAG GTA GCT GCA GA-3', with human *Sp1* as a reference gene. Amplification was done in LightCycler 480 Instrument II (Roche Diagnostics, Castle Hill,

NSW, Australia) with the following conditions: pre-denaturation at 95°C for 5 minutes, 50 cycles of 95°C for 10 seconds, 58°C for 10 seconds, and 72°C for 30 seconds with a single acquisition. Melt curve settings were 1 cycle of 95°C for 10 seconds, 60°C for 1 minute, and continuous at 97°C. Cycle threshold or crossing point values were calculated automatically, and values from the CRISPR/Cas9 mutants were subtracted from those of the Sp1 reference. The difference was plugged in equation $1/2^{(SP1-EGR1)}$. The obtained value was normalized to the CRISPR/Cas9 wild-type and multiplied by 2. Values between 1.5 and 2.5 were considered to have retained both alleles of *Egr-1* and therefore to be homozygously modified if the Sanger sequencing trace for the CRISPR/Cas9 mutants showed a single peak at the sites of mutation.

Conventional PCR

Amplification of longer human Egr-1 fragment was done using 50 ng genomic DNA with AccuPrime Pfx Supermix and final primer concentration of 0.2 μ M. Primers used were human Egr-1DFWD 5'-CTT CAA CCC TCA GGC GGA CA-3' and human Egr-1EREV 5'-GCC ACA TGT GAG AGT ACG GT-3'. Amplifications were performed in a PCR Thermal Cycler (Applied Biosystems, Foster City, CA) with an initial denaturation of 95°C for 5 minutes, 35 cycles of 95°C for 15 seconds, 58°C for 30 seconds, and 68°C for 2.5 minutes. The final PCR reactions were loaded into 0.8% agarose gels with 1 \times Tris-borate-EDTA running buffer. Gels were viewed and photographed using Molecular Imager Gel Doc XR (Bio-Rad Laboratories, Hercules, CA).

Western Blotting

CRISPR/Cas9 clones/cell types were seeded into 6-well plates, and at 80% to 90% confluency, cells were incubated in serum-free medium arrested for 24 hours. The cells were treated with a medium containing 5% FBS for 1 hour, then washed twice with cold 1 \times PBS before lysing with 1 \times RIPA buffer. Total protein samples were resolved by electrophoresis with denaturing SDS-polyacrylamide gels for 1 hour at 100 V. Proteins were transferred to Millipore Immobilon polyvinylidene difluoride membranes (Millipore, Burlington, MA) before incubation with 5% nonfat skim milk. Membranes were incubated with Egr-1 antibodies (Cell Signaling, Beverly, MA; cat. no. cs4153s) at a dilution of 1:1000. Mouse alpha tubulin antibodies (Sigma-Aldrich; cat. no. T5168) were used at a dilution of 1:40000 in 5% nonfat skim milk. Detection was achieved with horseradish peroxidase-linked secondary antibodies (1:2000 in 5% skim milk) and chemiluminescence (Perkin-Elmer, Waltham, MA).

Cell Adherence

Equal numbers of viable CRISPR/Cas9 clones/cell types (2×10^5 cells/well) in 10% FBS MCDB131 complete medium were seeded into 96-well plates and incubated for 2 hours. Adherent cells were trypsinized and counted using a Countess II automatic cell counter (Thermo Fisher Scientific).

Endothelial Proliferation by Cell Counting

CRISPR/Cas9 clones/cell types (3×10^3 viable cells/well) were seeded in 96-well plates. After 48 hours, cells were serum-deprived for 24 hours in MCDB131 medium that contained 10 ng/mL EGF (epidermal growth factor) (Sigma-Aldrich) and 1 μ g/mL hydrocortisone (Sigma-Aldrich), then further incubated in a medium containing 5% FBS, 10 ng/mL EGF (Sigma-Aldrich), and 1 μ g/mL hydrocortisone (Sigma-Aldrich). Cells were counted, and percent viability (Trypan blue exclusion) 72 hours after serum stimulation was determined using a Countess II automatic cell counter (Thermo Fisher Scientific). Forty-microliter cell suspension was mixed with an equal volume of 0.4% Trypan blue (Invitrogen; cat. no. T10282), and 10 μ L was loaded into Countess cell-counting chamber slides (Invitrogen; cat. no. C10283).

Cell Proliferation Using the xCELLigence System

The xCELLigence system (Roche Diagnostics) enables continuous, quantitative, and label-free assessment of cell growth.²⁷ CRISPR/Cas9 cell types (2×10^3 viable cells/well) were seeded in 96-well E-plates in complete MCDB131 medium containing 10% FBS, EGF (10 ng/mL; Sigma-Aldrich), and hydrocortisone (1 μ g/mL) and inserted into the xCELLigence RTCA station (Roche Diagnostics). Cell growth was automatically monitored every 15 minutes by the system. Cell index, a unitless parameter that reports the impedance of electron flow caused by adherent cells, represents a quantitative measure of cell growth in each well.

MTT Assay

The MTT assay provides a measure cellular metabolic activity and a surrogate measure of proliferation. CRISPR/Cas9 clones/cell types (2×10^3 viable cells/well) were seeded in 96-well plates and grown for 48 hours. Cells were incubated in serum-free medium for 24 hours before serum stimulation (5% FBS) for 48 hours. Ten microliters of MTT Labelling Reagent (Sigma-Aldrich) were added to each well (containing 100 μ L of medium), and the plates were incubated for 4 hours at 37°C before addition of 100 μ L of the solubilization solution. Overnight incubation was performed to ensure complete solubilization. Spectrophotometric

absorbance of the samples was measured at 550 nm, with 690 nm reference wavelength.

Endothelial Dual-Chamber Migration

CRISPR/Cas9 cell types (4×10^4 viable cells/well) in MCDB131 containing 10% FBS with complete growth supplements were seeded into the upper chamber of 24-well plates fitted with Millicell cell culture inserts (Millipore; cat. no. PI8P01250). After 24 hours, the medium was changed to 0.1% FBS serum, and the cells were left undisturbed for 24 hours. VEGF- A_{165} (25 ng/mL) (Sigma-Aldrich; cat. no. V7259) in 0.1% FBS was added to the lower chamber. After 24 hours, medium from the upper chamber was removed, and non-migrated cells and excess liquid were removed with a cotton swab. The cells were fixed in 70% ethanol for 10 minutes, and membranes were dried for 10 to 15 minutes. Filters were placed on slides and mounting medium (Fluoroshield with DAPI; Sigma; cat. no. 6057) was added. Specimens were visualized with an EVOS FL microscope. Images were taken at 10 \times magnification.

Endothelial Network Formation

CRISPR/Cas9 cell types (4×10^4 viable cells/well) in MCDB131 containing 1% FBS and 50 ng/mL FGF-2 were added to 96-well plates coated overnight at 4°C, with 100 μ L of growth factor-reduced reconstituted basement membrane matrix (Matrigel; Corning, Corning, NY; cat. no. 354230). Tubular network formation was observed after 6 hours and photographed under 40 \times using an Olympus (Tokyo, Japan) CKX41 microscope. The number of tubules formed was counted using ImageJ (National Institutes of Health, Bethesda, MD).

Apoptosis/Necrosis Assay by Flow Cytometry

CRISPR/Cas9 cell types (3×10^5 viable cells/well) were seeded into 6-well plates in MCDB131 containing 10% FBS. After 72 hours, the culture medium was removed, and the cells were washed with PBS. Accutase (STEMCELL Technologies, Cambridge, MA; cat. no. 07920) was used to detach the cells. The cells were washed and centrifuged at 300g for 5 minutes and resuspended at 1×10^6 cells/mL in 500 μ L of 1 \times binding buffer (annexin V-fluorescein isothiocyanate (FITC) Apoptosis Staining/Detection Kit; Abcam, Cambridge, UK; cat. no. ab14085). The cells were transferred to 12 \times 75-mm tubes and annexin V-FITC/propidium iodide was added and incubated for 5 minutes at 22°C, protected from light. Stained cell suspensions were analyzed by flow cytometry using a BD LSRFortessa X20 (BD Biosciences).

Vascular Endothelial Cadherin Expression

CRISPR/Cas9 cell types were grown in 25-cm² flasks in MCDB131 containing 10% FBS for 24 hours. The cells were washed in PBS, and Accutase (STEMCELL Technologies; cat. no. 07920) was used to detach the cells. The cells were washed and spun at 300g for 5 minutes, then resuspended (0.5×10^6 cells in 100 μ L) in 4% formaldehyde for 15 minutes at 22°C, and permeabilized in cold 90% methanol for 10 minutes on ice. After washing in PBS, the cells were incubated with 100 μ L diluted VE-cadherin (vascular endothelial cadherin) antibody (Cell Signaling Technology, Danvers, MA; cat. no. 2500) for 1 hour at 22°C. After washing again, the cells were incubated in 100 μ L of diluted fluorochrome-conjugated secondary antibody (goat anti-rabbit immunoglobulin G, Alexa Fluor 488 [Thermo Fisher Scientific; cat. no. A-11008]) for 30 minutes at 22°C. Stained cell populations were identified by gating preparations with or without antibody and analyzed by flow cytometry using a BD LSRFortessa X20 (BD Biosciences).

Statistical Analysis

Statistical analysis was performed as stated in the figure legends using GraphPad (San Diego, CA) Prism software, and significance was indicated by asterisk(s). Normality was assessed using Kolmogorov-Smirnov and Shapiro-Wilk test. If distribution was not normal, a Mann-Whitney or Kruskal-Wallis test was performed as appropriate. Normally distributed data were analyzed by Student *t* test or 1-way ANOVA, as appropriate. Plotted data are expressed as mean \pm SEM. An “n” indicates biological triplicates rather than technical triplicates. Differences were considered significant when $P \leq 0.05$. Where indicated, * $P \leq 0.05$, ** $P < 0.01$, *** $P < 0.001$, and **** $P < 0.0001$ are provided.

RESULTS

Generation and Validation of CRISPR/Cas9 HMEC-1 Clones

With the aim of elucidating the functional importance of Ser26 in human endothelial cells, a CRISPR/Cas9 strategy was used to introduce into HMEC-1, a point mutation in the codon encoding Ser26, changing it to Ala (Figure 1A). Screening by sequencing genomic DNA identified 3 separate clones each for wild-type and mutant (Ser26>Ala). We also identified 3 clones in which a premature stop codon effectively caused deletion in *Egr-1*. Forward and reverse sequencing of *Egr-1* gave well-defined sequences for *Egr-1* in wild-type (Figure S1A through S1C), mutant (Figure S2A through S2C), and deletion (Figure S3A through S3C). Quantitative PCR-based copy

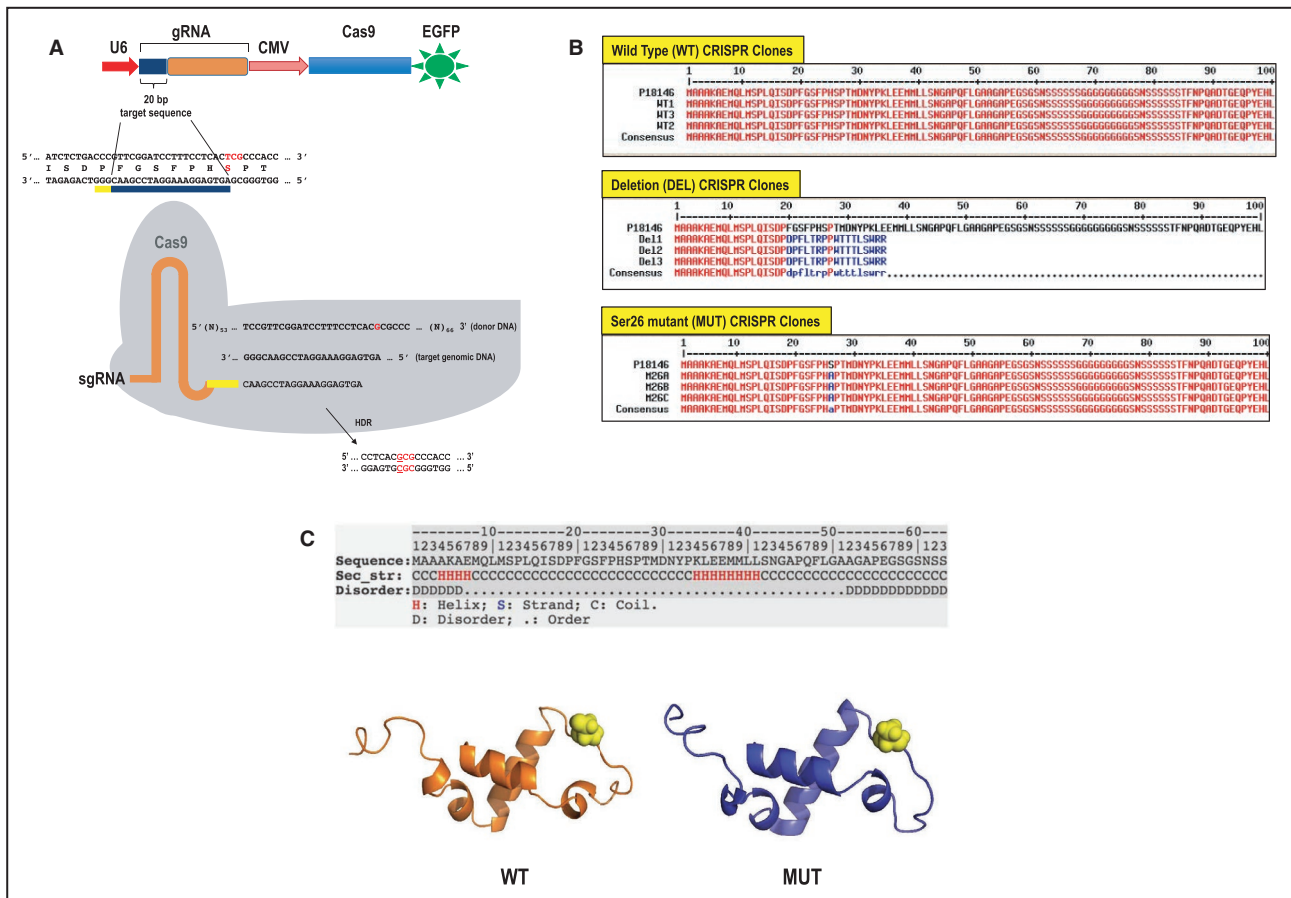


Figure 1. Generation and validation of CRISPR/Cas9 clones.

A, CRISPR/Cas9 strategy to introduce Egr-1 mutation. Using CRISPR/Cas9 single-guide RNA (sgRNA) guide design platform (<http://crispr.mit.edu>), a guide was selected that gave a high score and where protospacer adjacent motif (PAM) silent mutation was possible. A target on the reverse strand (indicated by the thick black line) was chosen and annealed oligonucleotides cloned into the PX458 (digested with *Bbs*I). The generated PX-458-Egr-1 was transfected into human microvascular endothelial cells together with the donor nucleotide to introduce a silent PAM mutation and point mutation of serine residue in Egr-1 at position 26 (Ser26)>Ala. This CRISPR/Cas9 system generated indels by nonhomologous end joining and the desired mutation via homology-directed repair (HDR). Transformants were sorted by fluorescence-activated cell sorting, and single cells with green fluorescent protein were grown and later screened. The target sequence (blue), not including the PAM site (yellow), was inserted into the guide RNA (gRNA). sgRNA contains the custom-designed sequence fused to the scaffold RNA sequence. Sequences of the target genomic DNA and donor oligonucleotide were shown. **B**, Alignment of amino acid sequences of different CRISPR/Cas9 clones with that of human Egr-1 (P18146). Multiple sequence alignment with hierarchical clustering was done using MultAlin software (<http://multalin.toulouse.inra.fr/multalin/>). **C**, In silico structure prediction by trRosetta of the amino-terminal region of Egr-1. The amino-terminus of the protein starts at the helix. The first 63 amino acid residues of Egr-1 were entered into trRosetta. Ser26 (yellow) is predicted to lie in a loop region between 2 helices. Wild-type (WT) (with Ser26) and mutant (MUT) (Ala26) Egr-1 sequence were run through the trRosetta program, and images were generated (using Pymol software). The WT model (shown in orange) was aligned structurally with the MUT model (blue). Residue 26 is highlighted in yellow. CVM indicates cytomegalovirus; Cas9, caspase 9; DEL, deletion; EGFP, enhanced green fluorescent protein; Egr-1, early growth response-1; and U6, the U6 promoter.

number analysis confirmed that the Ser26>Ala mutation was homozygous in mutant cells (Figure S4) and produced amplicons of correct size, suggesting no downstream insertion and/or deletion (Figure S5). Translation of nucleotide sequences and alignment with the human Egr-1 protein sequence (P18146) (Figure 1B) using MultAlin (<http://multalin.toulouse.inra.fr/multalin/>) revealed 100% homology for wild-type and only a Ser26>Ala change in mutant cells. The 4-nucleotide deletion in the 3 deletion clones

resulted in a frame shift causing premature termination (Figure S3).

In Silico Modeling of the Ser26>Ala Mutation

Ser26 resides near the amino terminus of Egr-1. In silico modeling of this region of the protein using trRosetta²⁸ predicts the N-terminus of Egr-1 and comprises a small globular domain of few short regions of helix. Ser26

resides in a solvent-exposed position in a loop linking 2 helical regions together (Figure 1C). Beyond this region, from approximately residue 60, Egr-1 is predicted to contain long disordered random coils with stretches of glycines and serines that suggest the amino-terminal region (containing Ser26) is isolated by a flexible tether from later regions such as the zinc fingers. Because a Ser26>Ala mutation is a mild mutation, in a loop, and solvent exposed, it is not expected the mutation perturbs the wild-type protein structure in this region (Figure 1C).

Effects of Ser26 Mutation and Egr-1 Deletion on Serum-Inducible Egr-1 Expression

Egr-1 is a serum-inducible immediate early gene product.^{12,29} Western blotting showed that Egr-1 (~75 kDa) is expressed in growth-quiescent wild-type and mutant cells exposed to medium containing 5% FBS for 1 hour (Figure 2). The induction of Egr-1 was more intense in wild-type cells than mutant cells. In contrast, Egr-1 was not detected in deletion cells (Figure 2).

Ser26 Mutation and Egr-1 Deletion Perturbs Endothelial Cell Proliferation

Cell proliferation assays were performed by stimulating growth with serum for 72 hours (Figure 3A). There was an 11-fold increase in the number of wild-type cells after this time. In contrast, proliferation of mutant cells or deletion cells increased by 2.6-fold, indicating that mutation of Ser26 or the absence of Egr-1 perturbed endothelial cell counts (Figure 3A). There was no significant difference in proliferation rate between mutant and deletion cells (Figure 3A). There was no difference in cell viability by Trypan blue exclusion after 72 hours (Figure 3B). To exclude the possibility that cell counts were merely

because of impaired attachment to the well surface among the cell types (although equal numbers of cells were seeded per well), we quantified the attached cells 2 hours after seeding. Figure 3C (left) demonstrates no difference in the extent of cell attachment among cell types, whereas Figure 3C (right) shows no difference in cell viability (by dye exclusion) after this time.

We performed further experiments using the xCELLigence system, in which wild-type, mutant, and deletion cells were seeded into E-plates, and growth was followed over time. There was no statistical difference between mutant and deletion growth, and both cell types grew slower than wild-type cells (Figure 4A). Similar results were obtained using the MTT assay, which provides a colorimetric assessment of metabolic activity (Figure 4B).

Ser26 Mutation and Egr-1 Deletion Ameliorates Endothelial Cell Migration

Knockdown studies have demonstrated a key role for Egr-1 in cell migration.^{30,31} To determine the importance of Ser26 in endothelial migration, we used a dual-chamber model in which cells traveled from the upper chamber toward VEGF-A₁₆₅ as a chemoattractant in the lower chamber. There was a 1.9-fold increase in the number of wild-type cells migrating toward VEGF-A₁₆₅. In contrast, there was a minor increase in migration (1.2-fold) by mutant or deletion cells. There was no difference in migration between mutant and deletion cells (Figure 5A and 5B).

Ser26 Mutation and Egr-1 Deletion Prevents Endothelial Network Formation

Network (or tubule) formation on solubilized basement membrane preparations is a widely used in vitro model of angiogenesis.³² Six hours after seeding each cell type, wild-type cells formed spontaneous networks on

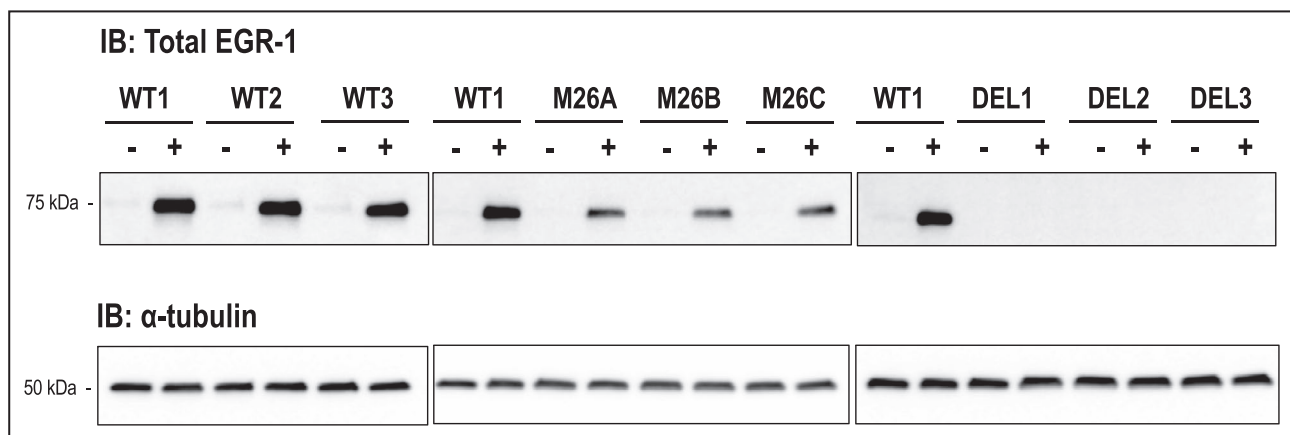


Figure 2. Induction by serum of Egr-1 in CRISPR/Cas9 clones.

Growth-quiescent wild-type (WT) (WT1, WT2, WT3), mutant (M) (M26A, M26B, M26C), and deletion (DEL) (DEL1, DEL2, DEL3) cells were treated with (+) or without (-) 5% FBS for 1 hour. Upper panels show total Egr-1 protein and lower panels correspond to α -tubulin. Approximate molecular weight markers are shown. Immunoblots are representative of 2 biologically independent experiments. Egr-1 indicates early growth response-1; and IB, immunoblotting.

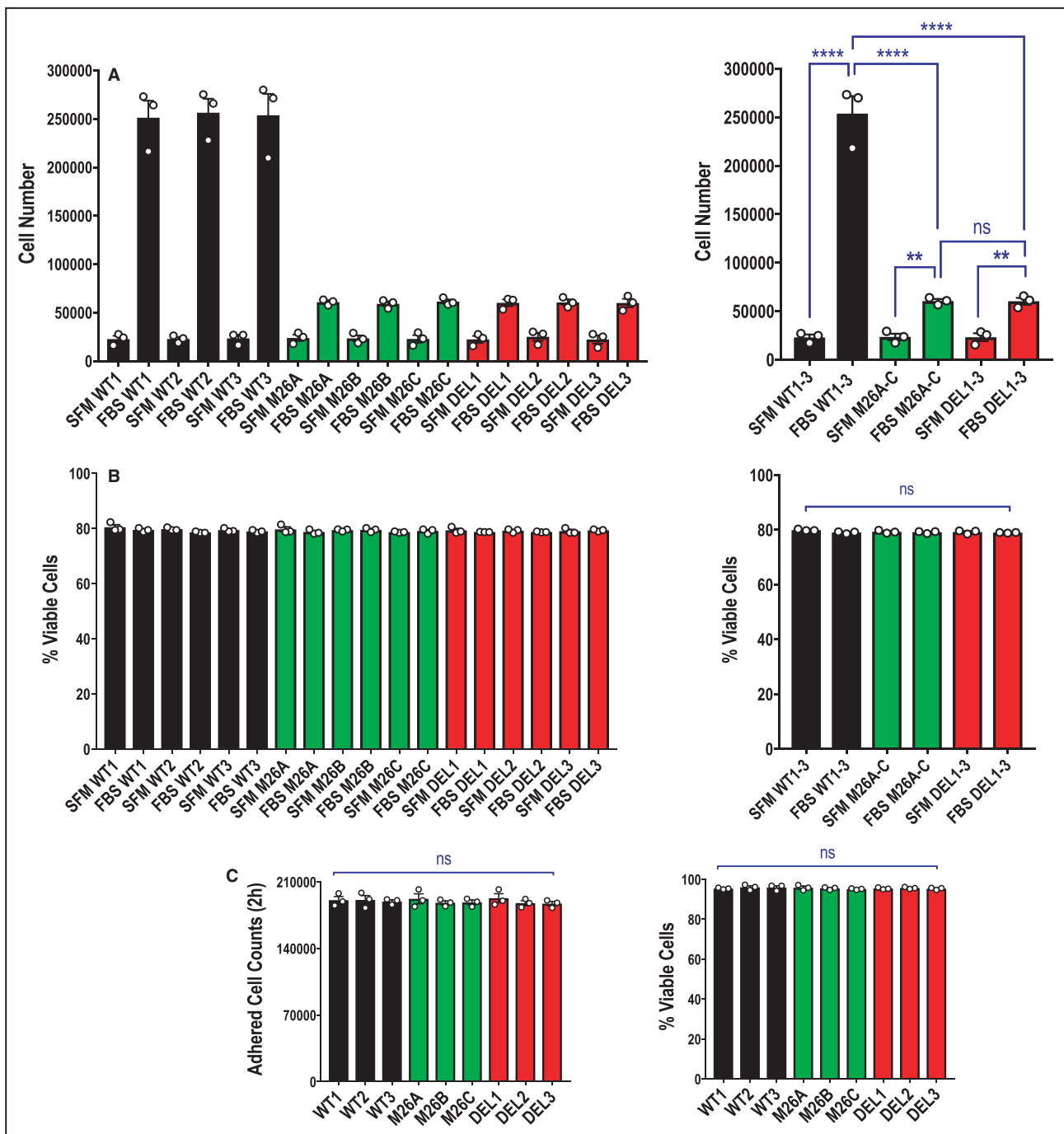


Figure 3. Effect of Ser26 mutation and Egr-1 deletion on endothelial cell total cell counts.

A, Proliferation assays were performed with CRISPR/Cas9 clones WT1, WT2, WT3, M26A, M26B, M26C, DEL1, DEL2, and DEL3 using the Countess II automated cell counter. Data represent the means of the means of 3 biologically independent experiments \pm SEM. Left, means of individual experiments. Right, combined means. Significance was assessed by 1-way ANOVA. ** $P < 0.01$; **** $P < 0.0001$. **B**, Viability of WT1, M26A, and DEL1 cells (from **A**) was determined after 72 hours when cell counts were quantified using the Countess II automatic cell counter with Trypan blue exclusion. Data represent the means of the means of 3 biologically independent experiments \pm SEM. Left, means of individual experiments. Right, combined means. Significance was assessed by Kruskal-Wallis test. **C**, Assessment of adherent cell counts (left) and viability (Trypan blue exclusion; right) of 3 clones per cell type 2 hours after 2×10^5 cells were seeded per well using the Countess II automatic cell counter. Data represent the means of the means of 3 biologically independent experiments \pm SEM. Significance was assessed by Kruskal-Wallis test or 1-way ANOVA. SFM denotes serum free medium; FBS denotes medium containing fetal bovine serum. DEL indicates deletion; Egr-1, early growth response-1; M, mutant; ns, not significant; and WT, wild-type.

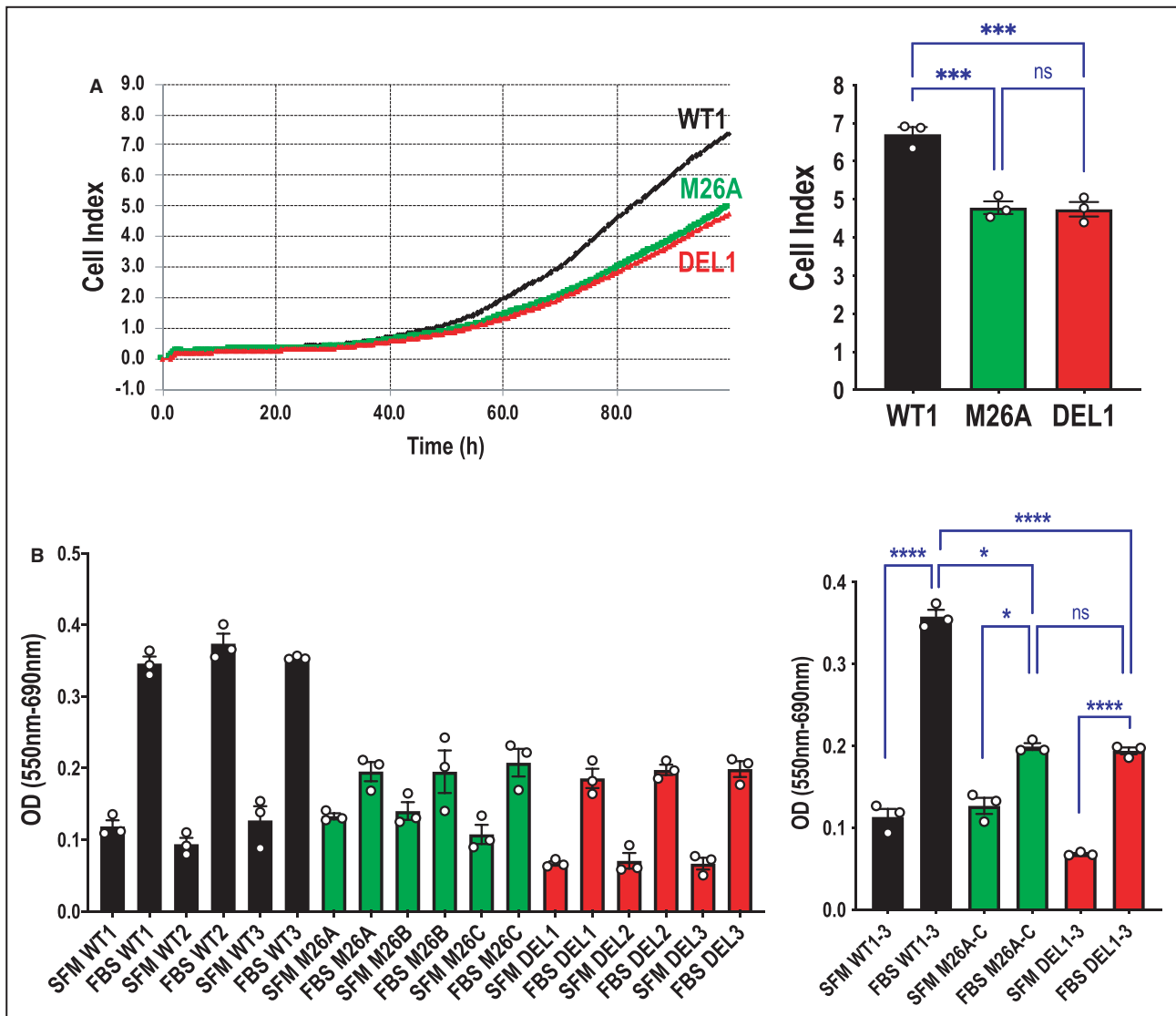


Figure 4. Effect of Ser26 mutation and Egr-1 deletion on real-time endothelial cell growth and metabolic activity.

A, Cell growth assays were performed using the xCELLigence system and WT1, M26A, and DEL1 cells. Data represent the means of the means of 3 biologically independent experiments \pm SEM. Left, representative xCELLigence real-time profile. Right, combined means 96 hours after seeding. Significance was assessed by 1-way ANOVA. *** P <0.001. **B**, MTT assays were performed with CRISPR/Cas9 clones WT1, WT2, WT3, M26A, M26B, M26C, DEL1, DEL2, and DEL3. Data represent the means of the means of 3 biologically independent experiments \pm SEM. Left, means of individual experiments. Right, combined means. Significance was assessed by Mann-Whitney or t test. * P <0.05. **** P <0.0001. SFM denotes serum free medium; FBS denotes medium containing fetal bovine serum. DEL indicates deletion; Egr-1, early growth response-1; M, mutant; ns, not significant; WT, wild-type; and OD, optical density.

Matrigel (with FGF-2). However, mutant and deletion cells formed networks 56% and 83% less efficiently than wild-type cells, respectively. Again, there was no difference in network formation between mutant and deletion cells (Figure 6A and 6B).

Ser26 Mutation and Egr-1 Deletion Elevates Endothelial Early and Late Apoptosis

We performed flow cytometry to determine levels of apoptosis among cell types. We were surprised to

detect dramatic differences in early (annexin V-FITC⁺/PI⁻) and late (annexin V-FITC⁺/PI⁺) apoptosis when comparing wild-type cells with mutant or deletion cells at 72 hours (Figure 7A and 7B). This contrasts with Trypan blue exclusion studies showing no difference among cell types (Figure 3B).

Ser26 Mutation and Egr-1 Deletion Elevates VE-Cadherin Expression

VE-cadherin is a well-established regulator of endothelial adhesion and signaling, permeability, and

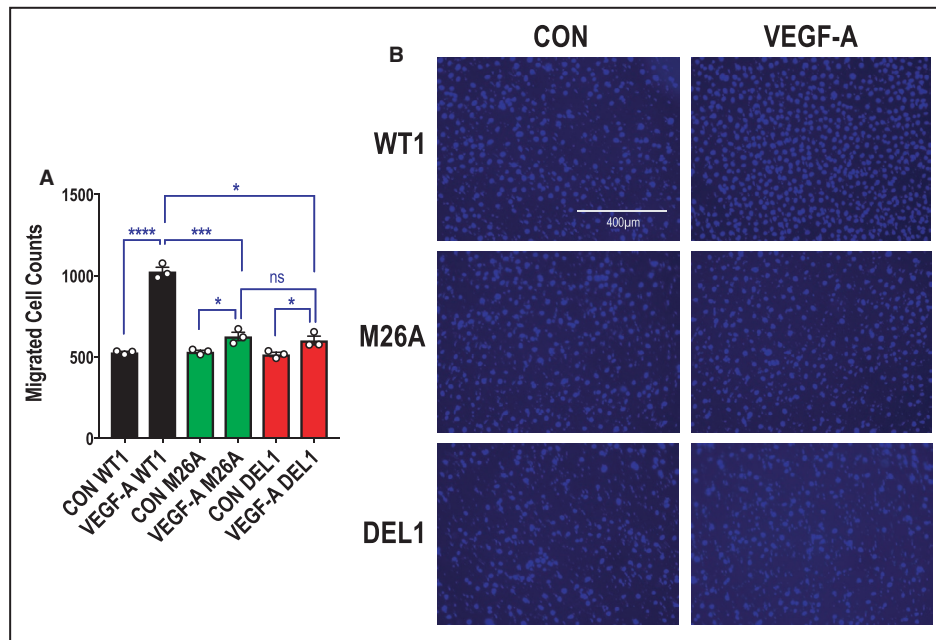


Figure 5. Effect of Ser26 mutation and Egr-1 deletion on endothelial migration.

A, Migration assays were performed with CRISPR/Cas9 clones WT1, M26A, and DEL1 using a dual-chamber model containing VEGF-A₁₆₅ (vascular endothelial growth factor-A) (25 ng/mL) in the lower chamber. Data represent the means of 3 biologically independent experiments \pm SEM. Significance was assessed by Mann-Whitney or *t* test. * $P \leq 0.05$; *** $P < 0.001$; **** $P < 0.0001$. **B**, Representative DAPI-stained nuclei in each condition. The cells were photographed under 10 \times magnification. CON indicates control cells (in 0.1% FBS) in the model without VEGF-A₁₆₅; DEL, deletion; Egr-1, early growth response-1; M, mutant; ns, not significant; and WT, wild-type.

angiogenesis.³³ Because VE-cadherin is negatively regulated by Egr-1,¹⁶ we hypothesized that levels of this master regulator of endothelial function would increase in HMEC-1 deficient in Egr-1. Flow cytometry revealed that VE-cadherin expression is weakly expressed in wild-type-1 cells, consistent with prior studies using HMEC-1,^{34,35} but considerably higher in deletion-1 and mutant-1 cells (Figure 8), indicating an inverse proportional relationship between Egr-1 (and Ser26 in Egr-1) and VE-cadherin expression.

DISCUSSION

Egr-1 regulates the expression of hundreds of genes in vascular endothelial cells¹⁶ and is pivotal in the control of a diverse range of biological processes in this and other cell types.¹⁷ For example, our own work has shown that Egr-1 is activated by vascular injury,¹⁵ fluid shear stress,⁸ phorbol esters,³⁶ and growth factors such as FGF-2,²⁴ and controls wound repair in vitro and injured arteries in rats^{13,37} and pigs.¹² Egr-1 also controls tumor angiogenesis in mice and corneal neovascularization in rats.² Egr-1 physically interacts with CREB1 (cAMP responsive element binding protein 1) and controls proangiogenic growth factors such

as VEGF-A₁₆₅, PGF (placental growth factor), HB-EGF (heparin-binding EGF-like growth factor) and PDGF (platelet-derived growth factor),³⁸ sustains high levels of phosphatase of activated cells 1, which mediates reactive oxygen species-dependent T-cell function,³⁹ positively regulates the superoxide dismutase 2 promoter,⁴⁰ recruits the DNA demethylase TET1 to remove methylation marks and activate downstream genes,⁴¹ mediates estrous cycle-dependent chromatin and transcriptional change,⁴² interacts with the receptor tyrosine kinase colony stimulating factor-1 receptor, which controls monocyte/macrophage generation,⁴³ and regulates stem/progenitor cell survival.⁴⁴ This recent work reiterates that Egr-1 serves a critical role in a wide range of biological processes in multiple cell types.^{17,19} However, our understanding of how cellular processes are influenced by Egr-1 phosphorylation, a critical epigenetic switch that can dramatically influence the activity of a protein,⁴⁵ is unclear. We recently identified a highly conserved serine residue in Egr-1 undergoing phosphorylation in human endothelial cells.²⁴ This article investigates the functional importance of Ser26 in Egr-1.

Here we used the CRISPR/Cas9 system to create a germline deletion in *Egr-1* in HMEC-1 to show that

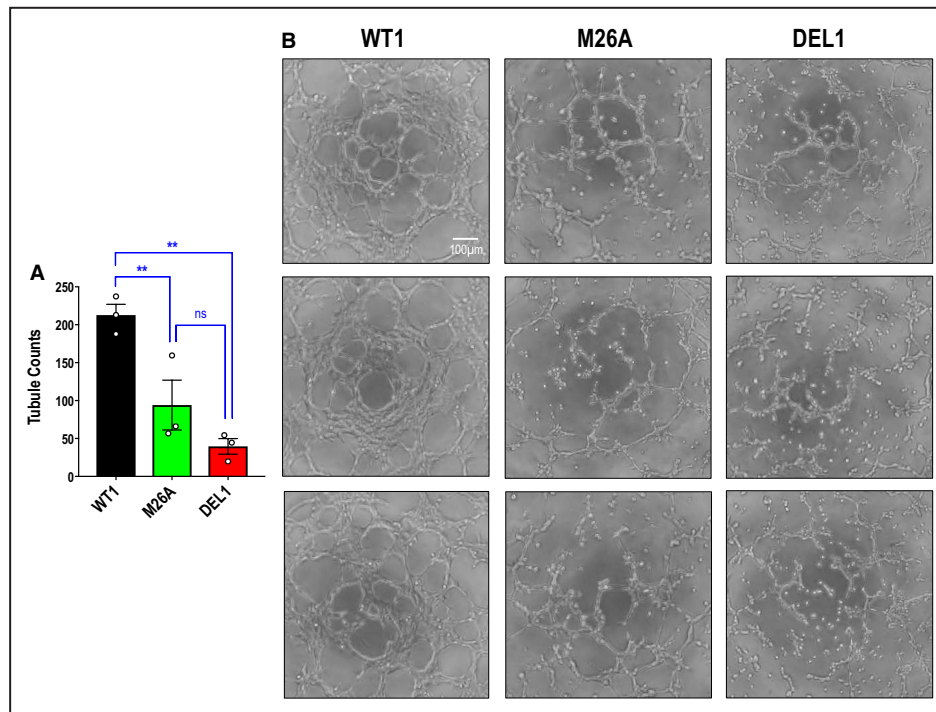


Figure 6. Effect of Ser26 mutation and Egr-1 deletion on endothelial network formation on Matrigel.

A, Network formation assays were performed with CRISPR/Cas9 clones WT1, M26A, and DEL1 in MCDB131 containing 1% FBS and 50 ng/mL FGF-2 (fibroblast growth factor-2) on a bed of Matrigel. Data represent the means of the means of 3 biologically independent experiments \pm SEM. Significance was assessed by 1-way ANOVA. $**P < 0.01$. **B**, Representative network formation. The cells were photographed under 40 \times magnification. Three separate fields are shown for each cell type. DEL indicates deletion; Egr-1; early growth response-1; M, mutant; ns, not significant; and WT, wild-type.

this transcription factor is not only critical for endothelial cell proliferation, migration, and network formation, but that a single-point mutation in Ser26 is sufficient to impair each of these cellular processes as effectively as the complete absence of Egr-1. HMEC-1 are transformed human endothelial lines, with characteristics akin to primary endothelial cells.⁴⁶ There was no difference in the ability of mutant and deletion cells to proliferate (whether basal growth or after serum induction), migrate in response to VEGF-A₁₆₅, or form networks on a solubilized basement membrane, because both of these cell types have reduced ability compared with wild-type cells. These are important findings because although on the one hand they confirm the reliance of endothelial cell proliferation, migration, and network formation on Egr-1, our data also indicate the reliance upon Ser26 in Egr-1 for each of these processes. This follows our demonstration that Egr-1 is inducibly expressed by serum in wild-type and mutant cells but not in deletion cells exposed to serum. Reduced inducible Egr-1 expression in mutant cells in response to FBS (Figure 2) may be caused by Egr-1 autoregulation with mutant Egr-1 noting that the

Egr-1 promoter contains nucleotide recognition elements for Egr-1.⁶

Wild-type, mutant, and deletion cells were used in experimental models involving multiple concentrations of FBS, some involving prior serum deprivation, to investigate effects on inducible Egr-1 expression or cell phenotype. Mutant and deletion cells showed similar effects (relative to wild-type) despite our use of serum prestarvation then 5% FBS (Countess, Figure 3A and 3B; MTT, Figure 4B), continuous 10% FBS without prestarvation (Countess, Figure 3C; xCELLigence, Figure 4A; apoptosis, Figure 7), or reduced FBS/agonist exposure (migration toward VEGF-A₁₆₅, Figure 5; network formation with FGF-2, Figure 6). This shows that the functional importance of Ser26 in Egr-1 is not confined to a particular experimental condition, and that the integrity of this highly conserved²⁴ residue in Egr-1 is as crucial as the presence of Egr-1 itself.

Although no difference in cell viability was detected among cell types using Trypan blue exclusion, flow cytometric analysis revealed that both early and late apoptosis increased when Ser26 was mutated or Egr-1 was deleted. The Trypan blue exclusion method

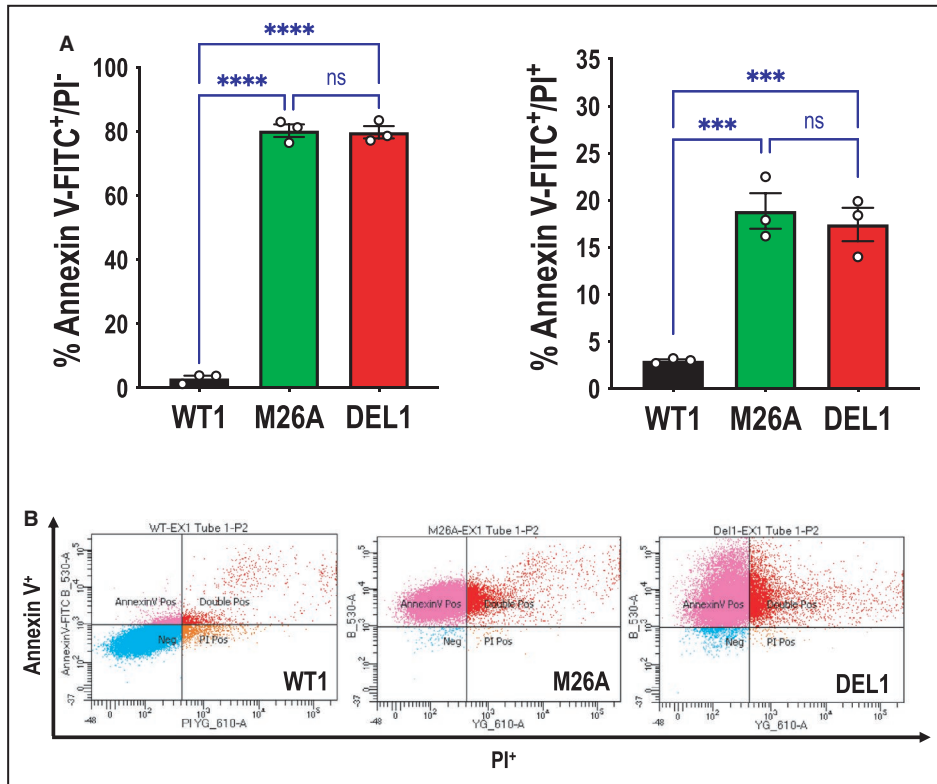


Figure 7. Effect of Ser26 mutation and Egr-1 deletion on endothelial early and late apoptosis.

A, Annexin V-FITC⁺/PI⁻ (left) or annexin V-FITC⁺/PI⁺ (right) staining comparing CRISPR/Cas9 clones WT1, M26A, and DEL1 in MCDB131 containing 10% FBS. Data represent the means of the means of 3 biologically independent experiments±SEM. Significance was assessed by 1-way ANOVA. ****P*<0.001; *****P*<0.0001. **B**, Representative annexin V-FITC⁺/PI⁻ and annexin V-FITC⁺/PI⁺ staining with WT1, M26A, and DEL1 cells by flow cytometry. Annexin V-FITC⁺/PI⁻ and annexin V-FITC⁺/PI⁺ reflect early and late apoptosis, respectively. DEL indicates deletion; Egr-1, early growth response-1; M, mutant; ns, not significant; and WT, wild-type.

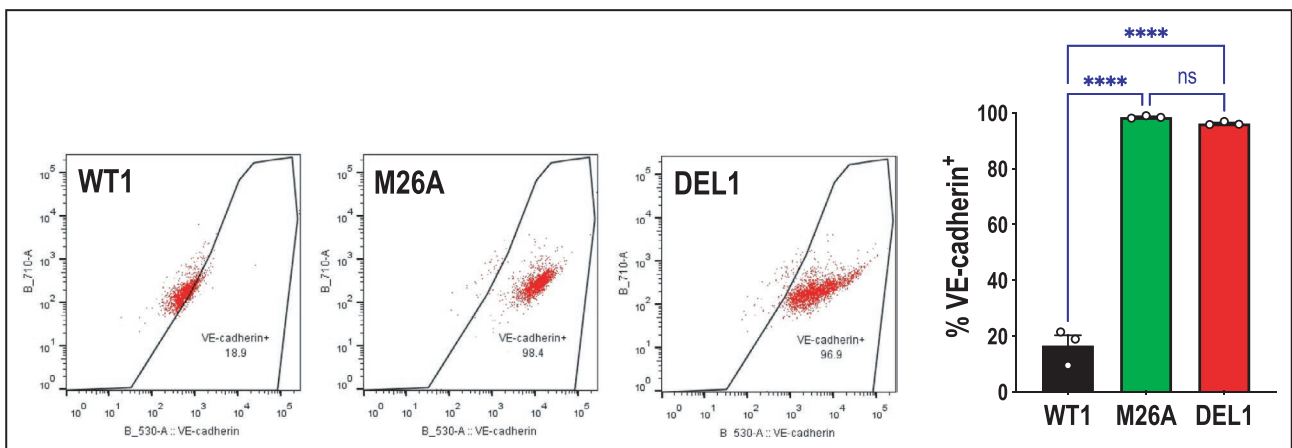


Figure 8. Effect of Ser26 mutation and Egr-1 deletion on VE-cadherin (vascular endothelial cadherin) expression.

VE-cadherin staining comparing CRISPR/Cas9 clones WT1, M26A, and DEL1 in MCDB131 containing 10% FBS. Data represent the means of the means of 3 biologically independent experiments±SEM. Significance was assessed by 1-way ANOVA. *****P*<0.0001. The figure shows representative VE-cadherin⁺ staining with WT1, M26A, and DEL1 cells by flow cytometry. DEL indicates deletion; M, mutant; ns, not significant; and WT, wild-type.

is commonly used to evaluate cytotoxicity in experimental investigations where dead or dying cells absorb dye into the cytoplasm because of loss of membrane integrity, with live cells remaining unstained, but this is less precise than flow cytometry.⁴⁷ Recent studies have found that Trypan blue can alter the morphology of dead cells, which causes dead cells to disappear and leads to overestimation of viability, a phenomenon not observed with propidium iodide staining.⁴⁸ We recently showed that suppression of Egr-1 expression can lead to apoptosis and reduced mitochondrial membrane potential.⁹ Our findings suggest that Egr-1, and in particular Ser26 in Egr-1, has protective effects preventing apoptosis, consistent with proproliferative, angiogenic, and reparative roles we previously described.^{2,14,30,49}

Limitations in this study include our use of an immortalized endothelial cell line, making uncertain as to whether identical mechanisms are operational in primary endothelial cells. HMEC-1 have nonetheless been used by many groups and retain many phenotypic, morphologic, and functional properties of normal human microvascular endothelial cells.^{50,51} A further limitation may be the apparent absence of a naturally occurring polymorphism or mutation in Egr-1 at Ser26 and its link with disease, vascular or otherwise. Conversely, the lack of a polymorphism or mutation at Ser26 and correlation with disease could indicate how critically important this highly conserved residue²⁴ is to the structure and function of Egr-1.

Wild-type, mutant, and deletion cells provide a new living resource for future research to gain further insights on how Egr-1 phosphorylation is controlled, how it can influence interactions with binding partners, and how it regulates other genes. For example, Egr-1 binds RelA, CBP, p300, or NAB1/2.¹⁷ It also interacts and competes with Sp1 in the promoter regions of PDGF-A, PDGF-B, transforming growth factor- β 1, urokinase-type plasminogen activator and tissue factor,¹⁵ and other promoters as observed by Huang et al,⁵² Thottassery et al,⁵³ Nebbaki et al,⁵⁴ Snyder et al,⁵⁵ and Su et al.⁵⁶ Egr-1 phosphorylation by CK2 (casein kinase 2) can reduce DNA-binding affinity and transcriptional activity⁵⁷ and results in less avid binding to Sp1 increasing colony-stimulating factor expression.⁵⁸ Our findings show that Ser26 in Egr-1, like Egr-1 itself, negatively controls VE-cadherin expression in line with prior work showing that Egr-1 suppresses VE-cadherin in endothelial¹⁶ and other cell types.⁵⁹ Wild-type, mutant, and deletion cells may therefore help better understand how Egr-1 phosphorylation links into gene-regulatory networks and alters the cell phenotype.

ARTICLE INFORMATION

Received December 13, 2020; accepted May 20, 2021.

Affiliation

Vascular Biology and Translational Research, School of Medical Sciences, UNSW Medicine and Health, University of New South Wales, Sydney, NSW, Australia.

Acknowledgments

The authors are grateful to A/Prof K. Quinlan and Dr G. Martyn (School of Biotechnology and Biomolecular Sciences, University of New South Wales Science) for advice on the generation of CRISPR cell lines. The authors acknowledge Dr K. Michie from the Structural Biology Facility (University of New South Wales Mark Wainwright Analytical Centre (which is funded in part by the Australian Research Council Linkage Infrastructure, Equipment and Facilities Grant: ARC LIEF 190100165) for assistance with the structural analysis of the Egr-1, Dr E. Johansson Beves and C. Brownlee (Flow Cytometry Facility, University of New South Wales Mark Wainwright Analytical Centre) for assistance with fluorescence-activated cell sorting analysis, and Dr J. Chan (Ramaciotti Centre for Genomics, University of New South Wales) for sequencing analysis. The authors also thank Prof I. Dawes for critical review of the article. Author contributions: Prof Khachigian conceptualized this project, interpreted data, directed experiments, and wrote the article. Drs Santiago and Li planned and performed experiments, analyzed and interpreted data, and wrote the article.

Sources of Funding

This work was supported by grants from the National Health and Medical Research Council of Australia (Program, Fellowship) and National Heart Foundation of Australia (Vanguard) (Prof Khachigian).

Disclosures

None.

Supplementary Material

Figures S1–S5

REFERENCES

- Crosby SD, Puetz JJ, Simburger KS, Fahrner TJ, Milbrandt J. The early response gene NGFI-C encodes a zinc finger transcriptional activator and is a member of the GCGGGGGCG (GSG) element-binding protein family. *Mol Cell Biol*. 1991;11:3835–3841. DOI: 10.1128/MCB.11.8.3835.
- Fahmy RG, Dass CR, Sun LQ, Chesterman CN, Khachigian LM. Transcription factor EGR-1 supports FGF-dependent angiogenesis during neovascularization and tumor growth. *Nature Med*. 2003;9:1026–1032. DOI: 10.1038/nm905.
- Day FL, Rafty LA, Chesterman CN, Khachigian LM. Angiotensin II (ATII)-inducible platelet-derived growth factor A-chain gene expression is p42/44 extracellular signal-regulated kinase-1/2 and Egr-1-dependent and mediated via the ATII type 1 but not type 2 receptor. induction by ATII antagonized by nitric oxide. *J Biol Chem*. 1999;274:23726–23733. DOI: 10.1074/jbc.274.34.23726.
- Delbridge GJ, Khachigian LM. Fgf-1-induced PDGF a-chain gene expression in vascular endothelial cells involves transcriptional activation by Egr-1. *Circ Res*. 1997;81:282–288.
- Yan SF, Mackman N, Kisiel W, Stern DM, Pinsky DJ. Hypoxia/hypoxemia-induced activation of the procoagulant pathways and the pathogenesis of ischemia-associated thrombosis. *Arterioscler Thromb Vasc Biol*. 1999;19:2029–2035. DOI: 10.1161/01.ATV.19.9.2029.
- Wang B, Chen J, Santiago FS, Janes M, Kavurma MM, Chong BH, Pimanda JE, Khachigian LM. Phosphorylation and acetylation of histone H3 and autoregulation by early growth response 1 mediate interleukin 1 β induction of early growth response 1 transcription. *Arterioscler Thromb Vasc Biol*. 2010;30:536–545.
- Grimbacher B, Aicher WK, Peter HH, Eibel H. TNF- α induces the transcription factor Egr-1, pro-inflammatory cytokines and cell proliferation in human skin fibroblasts and synovial lining cells. *Rheumatol Int*. 1998;17:185–192.
- Khachigian LM, Anderson KA, Halton NJ, Resnick N, Gimbrone MA Jr, Collins T. Egr-1 is activated in endothelial cells exposed to fluid shear stress and interacts with a novel shear-stress response element in the PDGF a-chain promoter. *Arterioscler Thromb Vasc Biol*. 1997;17:2280–2286.
- Billah M, Ridiandries A, Rayner BS, Allahwala UK, Dona A, Khachigian LM, Bhindi R. Egr-1 functions as a master switch regulator of remote

- ischemic preconditioning-induced cardioprotection. *Basic Res Cardiol*. 2019;115:3. DOI: 10.1007/s00395-019-0763-9.
10. Bhindi R, Fahmy RG, McMahon AC, Khachigian LM, Lowe HC. Intracoronary delivery of dnazymes targeting human Egr-1 reduces infarct size following myocardial ischaemia reperfusion. *J Pathol*. 2012;227:157–164. DOI: 10.1002/path.2991.
 11. Bhindi R, Khachigian LM, Lowe HC. Dnazymes targeting the transcription factor Egr-1 reduce myocardial infarct size following ischemia-reperfusion in rats. *J Thromb Haemost*. 2006;4:1479–1483. DOI: 10.1111/j.1538-7836.2006.02022.x.
 12. Lowe HC, Fahmy RG, Kavurma MM, Baker A, Chesterman CN, Khachigian LM. Catalytic oligodeoxynucleotides define a key regulatory role for early growth response factor-1 in the porcine model of coronary in-stent restenosis. *Circ Res*. 2001;89:670–677.
 13. Santiago FS, Lowe HC, Kavurma MM, Chesterman CN, Baker A, Atkins DG, Khachigian LM. New DNA enzyme targeting Egr-1 mRNA inhibits vascular smooth muscle proliferation and regrowth factor injury. *Nature Med*. 1999;5:1264–1269.
 14. Santiago FS, Lowe HC, Day FL, Chesterman CN, Khachigian LM. Early growth response factor-1 induction by injury is triggered by release and paracrine activation by fibroblast growth factor-2. *Am J Pathol*. 1999;154:937–944. DOI: 10.1016/S0002-9440(10)65341-2.
 15. Khachigian LM, Lindner V, Williams AJ, Collins T. Egr-1-induced endothelial gene expression: a common theme in vascular injury. *Science*. 1996;271:1427–1431. DOI: 10.1126/science.271.5254.1427.
 16. Fu M, Zhu X, Zhang J, Liang J, Lin Y, Zhao L, Ehrenguber MU, Chen YE. Egr-1 target genes in human endothelial cells identified by microarray analysis. *Gene*. 2003;315:33–41. DOI: 10.1016/S0378-1119(03)00730-3.
 17. Khachigian LM. Egr-1 in the pathogenesis of cardiovascular disease. *J Mol Med*. 2016;94:747–753. DOI: 10.1007/s00109-016-1428-x.
 18. Ramadas N, Rajaraman B, Kuppuswamy AA, Vedantham S. Early growth response-1 (EGR-1)—a key player in myocardial cell injury. *Cardiovasc Hematol Agents Med Chem*. 2014;12:66–71. DOI: 10.2174/1871525713666150123152131.
 19. Khachigian LM. Early growth response-1 in cardiovascular pathobiology. *Circ Res*. 2006;98:186–191. DOI: 10.2174/1871525713666150123152131.
 20. Arner E, Daub CO, Vitting-Seerup K, Andersson R, Lilje B, Drabløs F, Lennartsson A, Rønnerblad M, Hrydzusko O, Vitezic M, et al. Transcribed enhancers lead waves of coordinated transcription in transitioning mammalian cells. *Science*. 2015;347:1010–1014. DOI: 10.1126/science.1259418.
 21. Munoz-Chapuli R. Evolution of angiogenesis. *Int J Dev Biol*. 2011;55:345–351. DOI: 10.1387/ijdb.103212rm.
 22. Srinivasan R, Zabuawala T, Huang H, Zhang J, Gulati P, Fernandez S, Karlo JC, Landreth GE, Leone G, Ostrowski MC. Erk1 and Erk2 regulate endothelial cell proliferation and migration during mouse embryonic angiogenesis. *PLoS One*. 2009;4:e8283. DOI: 10.1371/journal.pone.0008283.
 23. Cao XM, Koski RA, Gashier A, McKiernan M, Morris CF, Gaffney R, Hay RV, Sukhatme VP. Identification and characterization of the egr-1 gene product, a DNA-binding zinc finger protein induced by differentiation and growth signals. *Mol Cell Biol*. 1990;10:1931–1939. DOI: 10.1128/MCB.10.5.1931.
 24. Santiago FS, Sanchez-Guerrero E, Zhang G, Zhong L, Raftery M, Khachigian LM. Extracellular signal-regulated kinase-1 phosphorylates early growth response-1 at serine 26. *Biochem Biophys Res Commun*. 2019;510:345–351. DOI: 10.1016/j.bbrc.2019.01.019.
 25. Yik JJ, Crossley M, Quinlan KGR. Chapter 15: genome editing of erythroid cell culture model systems. In: Lloyd JA, ed. *Erythropoiesis: Methods and Protocols, Methods and Molecular Biology*. Springer; 2018:245–257.
 26. Ran FA, Hsu PD, Wright J, Agarwala V, Scott DA, Zhang F. Genome engineering using the CRISPR-Cas9 system. *Nat Protoc*. 2013;8:2281–2308. DOI: 10.1038/nprot.2013.143.
 27. Li Y, Alhendi MN, Yeh MC, Elahy M, Santiago FS, Deshpande N, Wu B, Chan E, Inam S, Prado-Lourenco L, et al. Thermostable small molecule inhibitor of angiogenesis and vascular permeability that suppresses a pERK-FosB/ΔFosB-VCAM-1 axis. *Sci Adv*. 2020;6:eaz7815. DOI: 10.1126/sciadv.aaz7815.
 28. Yang J, Anishchenko I, Park H, Peng Z, Ovchinnikov S, Baker D. Improved protein structure prediction using predicted interresidue orientations. *Proc Natl Acad Sci USA*. 2020;117:1496–1503. DOI: 10.1073/pnas.1914677117.
 29. Fahmy RG, Khachigian LM. Antisense Egr-1 RNA driven by the CMV promoter is an inhibitor of vascular smooth muscle cell proliferation and regrowth after injury. *J Cell Biochem*. 2002;84:575–582. DOI: 10.1002/jcb.10057.
 30. Abdel-Malak NA, Mofarrahi M, Mayaki D, Khachigian LM, Hussain SN. Early growth response-1 regulates angiotensin-1-induced endothelial cell proliferation, migration, and differentiation. *Arterioscler Thromb Vasc Biol*. 2009;29:209–216. DOI: 10.1161/ATVBAHA.108.181073.
 31. Alhendi AMN, Patrikakis M, Daub CO, Kawaji H, Itoh M, de Hoon M, Carninci P, Hayashizaki Y, Arner E, Khachigian LM. Promoter usage and dynamics in vascular smooth muscle cells exposed to fibroblast growth factor-2 or interleukin-1β. *Sci Rep*. 2018;8:13164. DOI: 10.1038/s41598-018-30702-4.
 32. Montesano R, Orci L, Vassalli P. In vitro rapid organization of endothelial cells into capillary-like networks is promoted by collagen matrices. *J Cell Biol*. 1983;97:1648–1652. DOI: 10.1083/jcb.97.5.1648.
 33. Harris ES, Nelson WJ. Ve-cadherin: at the front, center, and sides of endothelial cell organization and function. *Curr Opin Cell Biol*. 2010;22:651–658. DOI: 10.1016/j.cob.2010.07.006.
 34. Evangelista K, Franco R, Schwab A, Coburn J. Leptospira interrogans binds to cadherins. *PLoS Negl Trop Dis*. 2014;8:e2672. DOI: 10.1371/journal.pntd.0002672.
 35. Oostingh GJ, Schlickum S, Friedl P, Schon MP. Impaired induction of adhesion molecule expression in immortalized endothelial cells leads to functional defects in dynamic interactions with lymphocytes. *J Invest Dermatol*. 2007;127:2253–2258. DOI: 10.1038/sj.jid.5700828.
 36. Khachigian LM, Williams AJ, Collins T. Interplay of Sp1 and Egr-1 in the proximal PDGF-α promoter in cultured vascular endothelial cells. *J Biol Chem*. 1995;270:27679–27686.
 37. Lowe HC, Chesterman CN, Khachigian LM. Catalytic antisense DNA molecules targeting Egr-1 inhibit neointima formation following permanent ligation of rat common carotid arteries. *Thromb Haemost*. 2002;87:134–140. DOI: 10.1055/s-0037-1612956.
 38. Kant S, Craige SM, Chen K, Reif MM, Learnard H, Kelly M, Caliz AD, Tran KV, Ramo K, Peters OM, et al. Neural JNK3 regulates blood flow recovery after hindlimb ischemia in mice via an Egr1/Creb1 axis. *Nat Commun*. 2019;10:4223. DOI: 10.1038/s41467-019-11982-4.
 39. Dan L, Liu L, Sun Y, Song J, Yin Q, Zhang G, Qi F, Hu Z, Yang Z, Zhou Z, et al. The phosphatase PAC1 acts as a T cell suppressor and attenuates host antitumor immunity. *Nat Immunol*. 2020;21:287–297. DOI: 10.1038/s41590-019-0577-9.
 40. Wang X, Lu J, Xie W, Lu X, Liang Y, Li M, Wang Z, Huang X, Tang M, Pfaff DW, et al. Maternal diabetes induces autism-like behavior by hyperglycemia-mediated persistent oxidative stress and suppression of superoxide dismutase 2. *Proc Natl Acad Sci USA*. 2019;116:23743–23752. DOI: 10.1073/pnas.1912625116.
 41. Sun Z, Xu X, He J, Murray A, Sun MA, Wei X, Wang X, McCoig E, Xie E, Jiang XI, et al. Egr1 recruits TET1 to shape the brain methylome during development and upon neuronal activity. *Nat Commun*. 2019;10:3892. DOI: 10.1038/s41467-019-11905-3.
 42. Jaric I, Rocks D, Grealley JM, Suzuki M, Kundakovic M. Chromatin organization in the female mouse brain fluctuates across the oestrous cycle. *Nat Commun*. 2019;10:2851. DOI: 10.1038/s41467-019-10704-0.
 43. Bencheikh L, Diop MK, Rivière J, Imanci A, Pierron G, Souquere S, Naimo A, Morabito M, Dussiot M, De Leeuw F, et al. Dynamic gene regulation by nuclear colony-stimulating factor 1 receptor in human monocytes and macrophages. *Nat Commun*. 2019;10:1935. DOI: 10.1038/s41467-019-09970-9.
 44. Pellicano F, Park L, Hopcroft LEM, Shah MM, Jackson L, Scott MT, Clarke CJ, Sinclair A, Abraham SA, Hair A, et al. hsa-mir183/EGR1-mediated regulation of E2F1 is required for CML stem/progenitor cell survival. *Blood*. 2018;131:1532–1544. DOI: 10.1182/blood-2017-05-783845.
 45. Schmidt C, Beilsten-Edmands V, Robinson CV. Insights into eukaryotic translation initiation from mass spectrometry of macromolecular protein assemblies. *J Mol Biol*. 2016;428:344–356. DOI: 10.1016/j.jmb.2015.10.011.
 46. Majewska A, Wilkus K, Brodaczewska K, Kieda C. Endothelial cells as tools to model tissue microenvironment in hypoxia-dependent pathologies. *Int J Mol Sci*. 2021;22:520. DOI: 10.3390/ijms22020520.

47. Tennant JR. Evaluation of the trypan blue technique for determination of cell viability. *Transplantation*. 1964;2:685–694. DOI: 10.1097/00007890-196411000-00001.
48. Chan LL, Rice WL, Qiu J. Observation and quantification of the morphological effect of trypan blue rupturing dead or dying cells. *PLoS One*. 2020;15:e0227950. DOI: 10.1371/journal.pone.0227950.
49. Gousseva N, Kugathasan K, Chesterman CN, Khachigian LM. Early growth response factor-1 mediates insulin-inducible vascular endothelial cell proliferation and regrowth after injury. *J Cell Biochem*. 2001;81:523–534. DOI: 10.1002/1097-4644(20010601)81:3<523:AID-JCB1066>3.0.CO;2-E.
50. Ades EW, Candal FJ, Swerlick RA, George VG, Summers S, Bosse DC, Lawley TJ. HMEC-1: establishment of an immortalized human microvascular endothelial cell line. *J Invest Dermatol*. 1992;99:683–690. DOI: 10.1111/1523-1747.ep12613748.
51. Muñoz-Vega M, Massó F, Páez A, Carreón-Torres E, Cabrera-Fuentes HA, Fragoso JM, Pérez-Hernández N, Martínez LO, Najib S, Vargas-Alarcón G, et al. Characterization of immortalized human dermal microvascular endothelial cells (HMEC-1) for the study of HDL functionality. *Lipids Health Dis*. 2018;17:44. DOI: 10.1186/s12944-018-0695-7.
52. Huang RP, Fan Y, Ni Z, Mercola D, Adamson ED. Reciprocal modulation between Sp1 and Egr-1. *J Cell Biochem*. 1997;66:489–499. DOI: 10.1002/(SICI)1097-4644(19970915)66:4<489:AID-JCB8>3.0.CO;2-H.
53. Thottassery JV, Sun D, Zambetti GP, Troutman A, Sukhatme VP, Schuetz EG, Schuetz JD. Sp1 and Egr-1 have opposing effects on the regulation of the RatPgp2/mdr1b gene. *J Biol Chem*. 1999;274:3199–3206. DOI: 10.1074/jbc.274.5.3199.
54. Nebbaki SS, El Mansouri FE, Afif H, Kapoor M, Benderdour M, Duval N, Pelletier JP, Martel-Pelletier J, Fahmi H. Egr-1 contributes to il-1-mediated down-regulation of peroxisome proliferator-activated receptor gamma expression in human osteoarthritic chondrocytes. *Arthritis Res Ther*. 2012;14:R69.
55. Snyder R, Thekkumkara T. Interplay between EGR1 and SP1 is critical for 13-cis retinoic acid-mediated transcriptional repression of angiotensin type 1A receptor. *J Mol Endocrinol*. 2013;50:361–374. DOI: 10.1530/JME-12-0154.
56. Su T, Liu P, Ti X, Wu S, Xue X, Wang Z, Dioum E, Zhang Q. HIF1alpha, egr1 and sp1 co-regulate the erythropoietin receptor expression under hypoxia: an essential role in the growth of non-small cell lung cancer cells. *Cell Commun Signal*. 2019;17:152. DOI: 10.1186/s12964-019-0458-8.
57. Jain N, Mahendran R, Philp R, Guy GR, Tan YH, Cao X. Casein kinase II associates with Egr-1 and acts as a negative modulator of its DNA binding and transcription activities in NIH 3T3 cells. *J Biol Chem*. 1996;271:13530–13536. DOI: 10.1074/jbc.271.23.13530.
58. Srivastava S, Weitzmann MN, Kimble RB, Rizzo M, Zahner M, Milbrandt J, Ross FP, Pacifici R. Estrogen blocks M-CSF gene expression and osteoclast formation by regulating phosphorylation of Egr-1 and its interaction with Sp-1. *J Clin Invest*. 1998;102:1850–1859. DOI: 10.1172/JCI4561.
59. Mourad-Zeidan AA, Melnikova VO, Wang H, Raz A, Bar-Eli M. Expression profiling of Galectin-3-depleted melanoma cells reveals its major role in melanoma cell plasticity and vasculogenic mimicry. *Am J Pathol*. 2008;173:1839–1852. DOI: 10.2353/ajpath.2008.080380.

SUPPLEMENTARY INFORMATION

Serine 26 in Early Growth Response-1 is Critical for Endothelial Proliferation, Migration and Network Formation

Fernando S. Santiago, Yue Li and Levon M. Khachigian

Fig S1. Sequences and chromatographs from sequenced WT cells.

Alignment of *Egr-1* nucleotide sequences in WT cells with human *Egr-1* (NM_001964.3). Forward sequences are shown in the left upper panel while reverse complement sequences are shown in the upper right panel. The red box indicates the location of TCG (Ser26). Lower panels show the sequencing data. The translated amino acid sequence (partial) is shown. **A**, WT1; **B**, WT1; **C**, WT3 cells.

Fig S2. Sequences and chromatographs from sequenced MUT cells.

Alignment *Egr-1* nucleotide sequences in MUT cells with human *Egr-1* (NM_001964.3). Forward sequences are shown in the left upper panel while reverse complement sequences are shown in the upper right panel. The red box indicates the location of the TCG>GCG mutation (Ser26>Ala26). TCG (Ser26). Lower panels show the sequencing data. Green box indicates the location of silent PAM site. The translated amino acid sequence (partial), including the Ser26>Ala mutation (in red) is shown. **A**, M26A; **B**, M26B; **C**, M26C cells.

Fig S3. Sequences and chromatographs from sequenced DEL cells.

Alignment *Egr-1* nucleotide sequences in MUT cells with human *Egr-1* (P18146). Forward sequences are shown in the left upper panel while reverse complement sequences are shown in the upper right panel. Red box indicates the location of TCG (Ser26) in the reference sequence. Black box indicates the location of the 4-nucleotide deletion. Lower panels show the sequencing data. The translated amino acid sequence is shown, including nonsense sequences (in red, due to frameshift) and premature termination (*). **A**, DEL1; **B**, DEL2; **C**, DEL3 cells.

Fig S4. Copy number analysis in WT and M26 cells.

Copy number was determined by quantitative real-time PCR across the *Egr-1* region and Ct values were normalized against Ct values for PCR across a control gene (*Sp1*).

Fig S5. PCR of CRISPR/Cas9 clones.

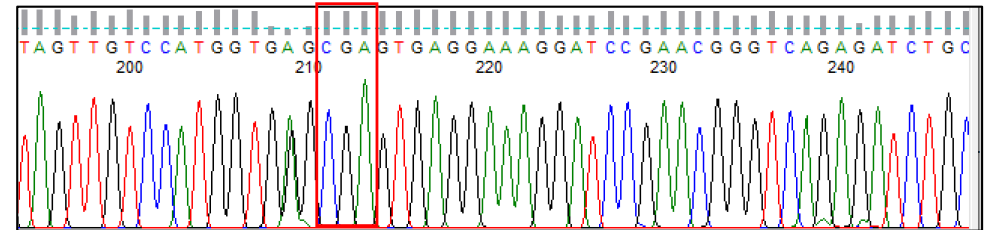
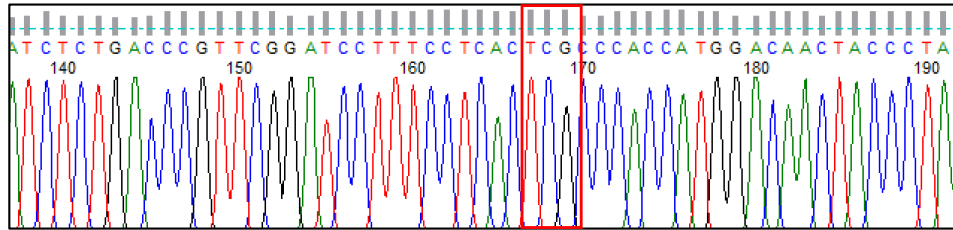
Long PCR of human *Egr-1* to test for insertions or indels downstream of Ser26. DNA size markers are shown.

Forward WT1

```
Query 70 CTCTCCAGCCTGCTCGTCCAGGATGGCCGCGGCCAAGGCCGAGATGCAGCTGATGTCCCC 129
Sbjct 262 CTCTCCAGCCTGCTCGTCCAGGATGGCCGCGGCCAAGGCCGAGATGCAGCTGATGTCCCC 321
Query 130 GCTGCAGATCTCTGACCCGTTTCGGATCCTTTCTCACTCGCCACCATGGACAACACTACCC 189
Sbjct 322 GCTGCAGATCTCTGACCCGTTTCGGATCCTTTCTCACTCGCCACCATGGACAACACTACCC 381
Query 190 TAAGCTGGAGGAGATGATGCTGCTGAGCAACGGGGCTCCCCAGTTCCTCGGCGCCGCCGG 249
Sbjct 382 TAAGCTGGAGGAGATGATGCTGCTGAGCAACGGGGCTCCCCAGTTCCTCGGCGCCGCCGG 441
```

Reverse Complement WT1

```
Query 124 CTGCTCGTCCAGGATGGCCGCGGCCAAGGCCGAGATGCAGCTGATGTCCCCGCTGCAGAT 183
Sbjct 271 CTGCTCGTCCAGGATGGCCGCGGCCAAGGCCGAGATGCAGCTGATGTCCCCGCTGCAGAT 330
Query 184 CTCTGACCCGTTTCGGATCCTTTCTCACTCGCTCACCATGGACAACACTACCCCTAAGCTGGA 243
Sbjct 331 CTCTGACCCGTTTCGGATCCTTTCTCACTCGCTCACCATGGACAACACTACCCCTAAGCTGGA 390
Query 244 GGAGATGATGCTGCTGAGCAACGGGGCTCCCCAGTTCCTCGGCGCCGCCGGGGCCCCAGA 303
Sbjct 391 GGAGATGATGCTGCTGAGCAACGGGGCTCCCCAGTTCCTCGGCGCCGCCGGGGCCCCAGA 450
```



MAAKAEMQLMSPLQISDPFGSFPHSPTMDNYPKLEEMLLSNGAPQFLGAAGAP
EGSGSNSSSSSSSGGGGGGGGGSNSSSSSSSTFNPQADTGEQPYEHL

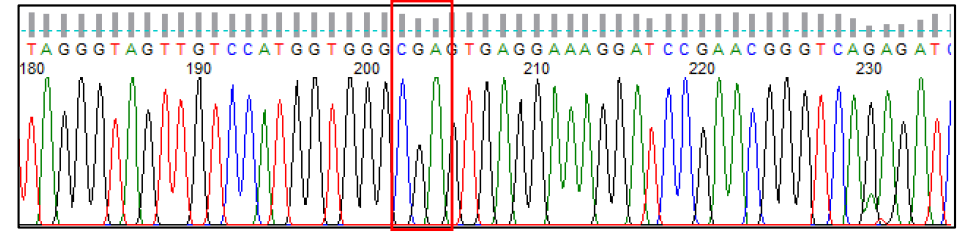
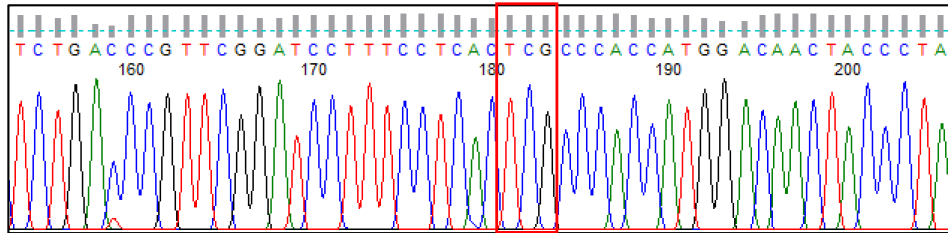
FIG. S1A

Forward WT2

Query	90	AGCCTGCTCGTCCAGGATGGCCGCGGCCAAGGCCGAGATGCAGCTGATGTCCCCGCTGCA	149
Sbjct	268	AGCCTGCTCGTCCAGGATGGCCGCGGCCAAGGCCGAGATGCAGCTGATGTCCCCGCTGCA	327
Query	150	GATCTCTGACCCGTTTCGGATCCTTTCTCACTCGGCCACCATGGACAACACCCTAAGCT	209
Sbjct	328	GATCTCTGACCCGTTTCGGATCCTTTCTCACTCGGCCACCATGGACAACACCCTAAGCT	387
Query	210	GGAGGAGATGATGCTGCTGAGCAACGGGGCTCCCCAGTTCCTCGGCGCCGCCGGGGCCCC	269
Sbjct	388	GGAGGAGATGATGCTGCTGAGCAACGGGGCTCCCCAGTTCCTCGGCGCCGCCGGGGCCCC	447

Reverse Complement WT2

Query	136	CAGGATGGCCGCGGCCAAGGCCGAGATGCAGCTGATGTCCCCGCTGCAGATCTTGACCC	195
Sbjct	280	CAGGATGGCCGCGGCCAAGGCCGAGATGCAGCTGATGTCCCCGCTGCAGATCTTGACCC	339
Query	196	GTTTCGGATCCTTTCTCACTCGGCCACCATGGACAACACCCTAAGCTGGAGGAGATGAT	255
Sbjct	340	GTTTCGGATCCTTTCTCACTCGGCCACCATGGACAACACCCTAAGCTGGAGGAGATGAT	399
Query	256	GCTGCTGAGCAACGGGGCTCCCCAGTTCCTCGGCGCCGCCGGGGCCCCAGAGGGcagcgg	315
Sbjct	400	GCTGCTGAGCAACGGGGCTCCCCAGTTCCTCGGCGCCGCCGGGGCCCCAGAGGGCAGCGG	459



MAAKAEMQLMSPLQISDPFGSFPHSPTMDNYPKLEEMLLSNGAPQFLGAAGAP
 EGSGSNSSSSSSSGGGGGGGGGSNSSSSSSSTFNPQADTGEQPYEHL

FIG. S1B

Forward WT3

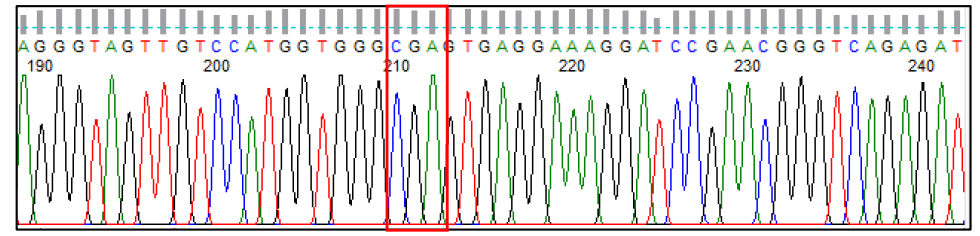
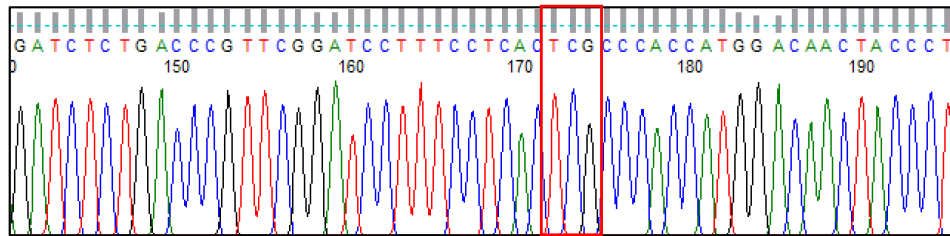
```

Query 71  CCAGCTCTCCAGCCTGCTCGTCCAGGATGGCCGCGGCCAAGGCCGAGATGCAGCTGATGT 130
Sbjct 258  CCAGCTCTCCAGCCTGCTCGTCCAGGATGGCCGCGGCCAAGGCCGAGATGCAGCTGATGT 317
Query 131  CCCCCTGCAGATCTCTGACCCGTTTCGGATCCTTTCTCACTCGCCACCATGGACAAC 190
Sbjct 318  CCCCCTGCAGATCTCTGACCCGTTTCGGATCCTTTCTCACTCGCCACCATGGACAAC 377
Query 191  ACCCTAAGCTGGAGGAGATGATGCTGCTGAGCAACGGGGCTCCCCAGTTCTCGGCGCCG 250
Sbjct 378  ACCCTAAGCTGGAGGAGATGATGCTGCTGAGCAACGGGGCTCCCCAGTTCTCGGCGCCG 437
  
```

Reverse Complement WT3

```

Query 138  CAGGATGGCCGCGGCCAAGGCCGAGATGCAGCTGATGTCCCCGCTGCAGATCTCTGACCC 197
Sbjct 280  CAGGATGGCCGCGGCCAAGGCCGAGATGCAGCTGATGTCCCCGCTGCAGATCTCTGACCC 339
Query 198  GTTCGGATCCTTTCTCACTCGCCACCATGGACAACACTACCCTAAGCTGGAGGAGATGAT 257
Sbjct 340  GTTCGGATCCTTTCTCACTCGCCACCATGGACAACACTACCCTAAGCTGGAGGAGATGAT 399
Query 258  GCTGCTGAGCAACGGGGCTCCCCAGTTCTCGGCGCCGCGGGGCCCCAGAgggcagcgg 317
Sbjct 400  GCTGCTGAGCAACGGGGCTCCCCAGTTCTCGGCGCCGCGGGGCCCCAGAGGGCAGCGG 459
  
```



MAAKAEMQLMSPLQISDPFGSFPHSPTMDNYPKLEEMMLLSNGAPQFLGAAGAP
 EGSGSNSSSSSSSGGGGGGGGGSNSSSSSSSTFNPQADTGEQPYEHLTQKDFI

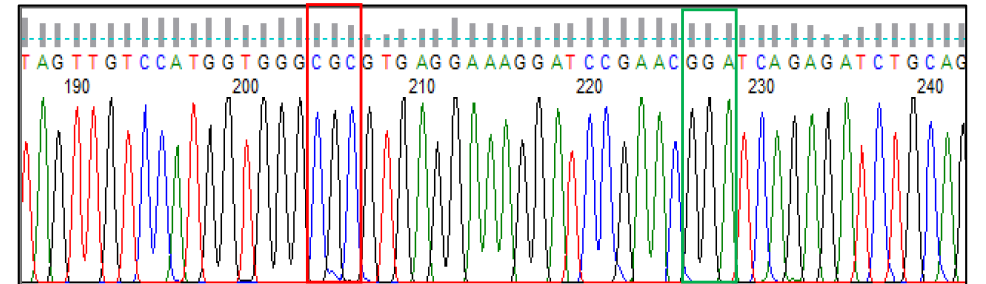
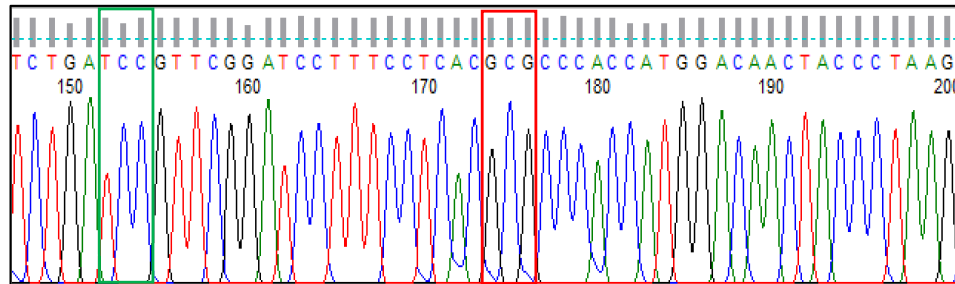
FIG. S1C

Forward M26A

Query	68	CGACACCAGCTCTCCAGCCTGCTCGTCCAGGATGGCCGCGGCCAAGGCCGAGATGCAGCT	127
Sbjct	253	CGACACCAGCTCTCCAGCCTGCTCGTCCAGGATGGCCGCGGCCAAGGCCGAGATGCAGCT	312
Query	128	GATGTCCCCGCTGCAGATCTCTGATCCGTTTCGGATCCTTTCCTCACGCGCCACCATGGA	187
Sbjct	313	GATGTCCCCGCTGCAGATCTCTGATCCCGTTTCGGATCCTTTCCTCACGCGCCACCATGGA	372
Query	188	CAACTACCCTAAGCTGGAGGAGATGATGCTGCTGAGCAACGGGGCTCCCCAGTTCCTCGG	247
Sbjct	373	CAACTACCCTAAGCTGGAGGAGATGATGCTGCTGAGCAACGGGGCTCCCCAGTTCCTCGG	432

Reverse Complement M26A

Query	132	CAGGATGGCCGCGGCCAAGGCCGAGATGCAGCTGATGTCCCCGCTGCAGATCTCTGATCC	191
Sbjct	280	CAGGATGGCCGCGGCCAAGGCCGAGATGCAGCTGATGTCCCCGCTGCAGATCTCTGATCC	339
Query	192	GTTTCGGATCCTTTCCTCACGCGCCACCATGGACAACACCCTAAGCTGGAGGAGATGAT	251
Sbjct	340	GTTTCGGATCCTTTCCTCACGCGCCACCATGGACAACACCCTAAGCTGGAGGAGATGAT	399
Query	252	GCTGCTGAGCAACGGGGCTCCCCAGTTCCTCGGCGCCGCGGGGCCCCAGAGggcagcgg	311
Sbjct	400	GCTGCTGAGCAACGGGGCTCCCCAGTTCCTCGGCGCCGCGGGGCCCCAGAGGGCAGCGG	459



MAAKAEMQLMSPLQISDPFGSFPHAPTMDNYPKLEEMLLSNGAPQFLGAAGAP
 EGSGSNSSSSSSGGGGGGGGGSNSSSSSSTFNPQADTGEQPYEHL

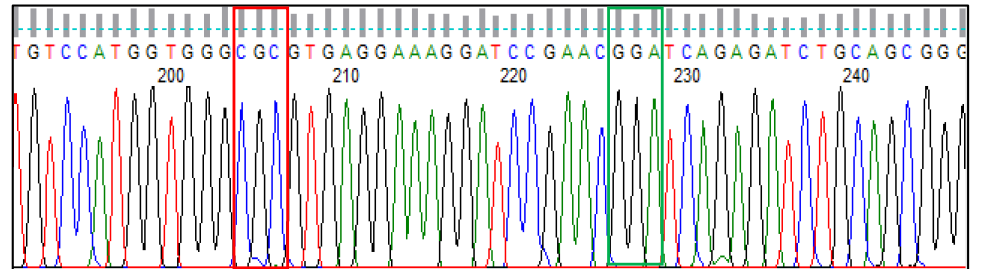
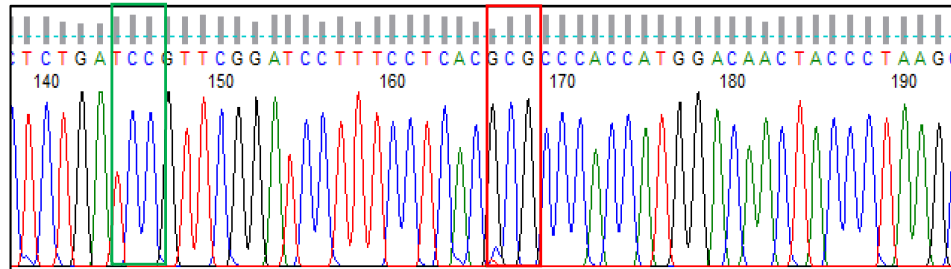
FIG. S2A

Forward M26B

Query	68	GCTCTCCAGCCTGCTCGTCCAGGATGGCCGCGGCCAAGGCCGAGATGCAGCTGATGTCCC	127
Sbjct	261	GCTCTCCAGCCTGCTCGTCCAGGATGGCCGCGGCCAAGGCCGAGATGCAGCTGATGTCCC	320
Query	128	CGCTGCAGATCTCTGATCCGTTTCGGATCCTTTCTCACGCGCCACCATGGACAACACTACC	187
Sbjct	321	CGCTGCAGATCTCTGATCCGTTTCGGATCCTTTCTCACGCGCCACCATGGACAACACTACC	380
Query	188	CTAAGCTGGAGGAGATGATGCTGCTGAGCAACGGGGCTCCCCAGTTCCTCGGCGCCGCCG	247
Sbjct	381	CTAAGCTGGAGGAGATGATGCTGCTGAGCAACGGGGCTCCCCAGTTCCTCGGCGCCGCCG	440

Reverse Complement M26B

Query	122	TGCTCGTCCAGGATGGCCGCGGCCAAGGCCGAGATGCAGCTGATGTCCCCGCTGCAGATC	181
Sbjct	272	TGCTCGTCCAGGATGGCCGCGGCCAAGGCCGAGATGCAGCTGATGTCCCCGCTGCAGATC	331
Query	182	TCTGATCCGTTTCGGATCCTTTCTCACGCGCCACCATGGACAACACTACCCTAAGCTGGAG	241
Sbjct	332	TCTGATCCGTTTCGGATCCTTTCTCACGCGCCACCATGGACAACACTACCCTAAGCTGGAG	391
Query	242	GAGATGATGCTGCTGAGCAACGGGGCTCCCCAGTTCCTCGGCGCCGCCGGGGCCCCAGAG	301
Sbjct	392	GAGATGATGCTGCTGAGCAACGGGGCTCCCCAGTTCCTCGGCGCCGCCGGGGCCCCAGAG	451



MAAKAEMQLMSPLQISDPFGSFP~~A~~PTMDNYPKLEEMLLSNGAPQFLGAAGAP
 EGSGSNSSSSSSSGGGGGGGGGSNSSSSSSSTFNPQADTGEQPYEHL

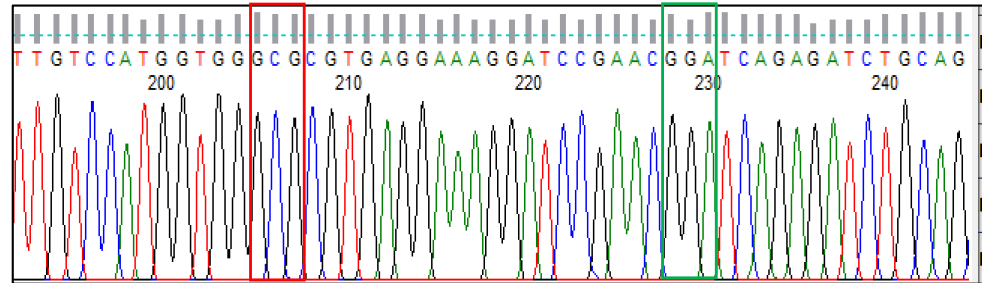
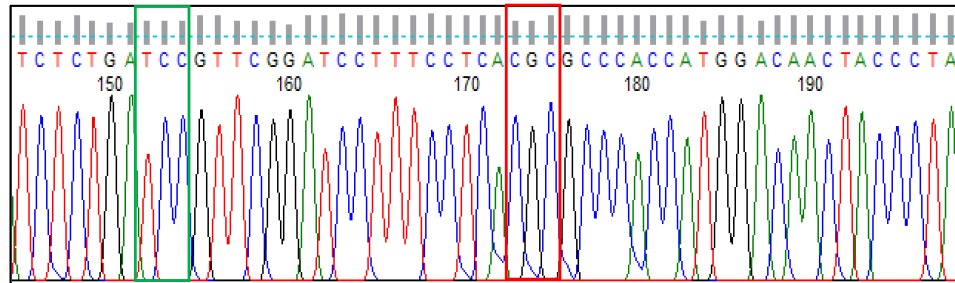
FIG. S2B

Forward M26C

Query	85	CCTGCTCGTCCAGGATGGCCGCGGCCAAGGCCGAGATGCAGCTGATGTCCCCGCTGCAGA	144
Sbjct	270	CCTGCTCGTCCAGGATGGCCGCGGCCAAGGCCGAGATGCAGCTGATGTCCCCGCTGCAGA	329
Query	145	TCTCTGATCCGTTTCGGATCCTTTCTCACTCGCCACCATGGACAACCTACCCTAAGCTGG	204
Sbjct	330	TCTCTGATCCGTTTCGGATCCTTTCTCACTCGCCACCATGGACAACCTACCCTAAGCTGG	389
Query	205	AGGAGATGATGCTGCTGAGCAACGGGGCTCCCCAGTTCTCGGCGCCGCCGGGGCCCCAG	264
Sbjct	390	AGGAGATGATGCTGCTGAGCAACGGGGCTCCCCAGTTCTCGGCGCCGCCGGGGCCCCAG	449

Reverse Complement M26C

Query	75	GCTCCAGCCCCGGGCTGCACccccccGCCCCGACACCAGCTCTCCAGCCTGCTCGTCCAG	134
Sbjct	223	GCTCCAGCCCCGGGCTGCACCCCCCGCCCCGACACCAGCTCTCCAGCCTGCTCGTCCAG	282
Query	135	GATGGCCGCGGCCAAGGCCGAGATGCAGCTGATGTCCCCGCTGCAGATCTCTGATCCCGTT	194
Sbjct	283	GATGGCCGCGGCCAAGGCCGAGATGCAGCTGATGTCCCCGCTGCAGATCTCTGATCCCGTT	342
Query	195	CGGATCCTTTCTCACTCGCCACCATGGACAACCTACCCTAAGCTGGAGGAGATGATGCT	254
Sbjct	343	CGGATCCTTTCTCACTCGCCACCATGGACAACCTACCCTAAGCTGGAGGAGATGATGCT	402

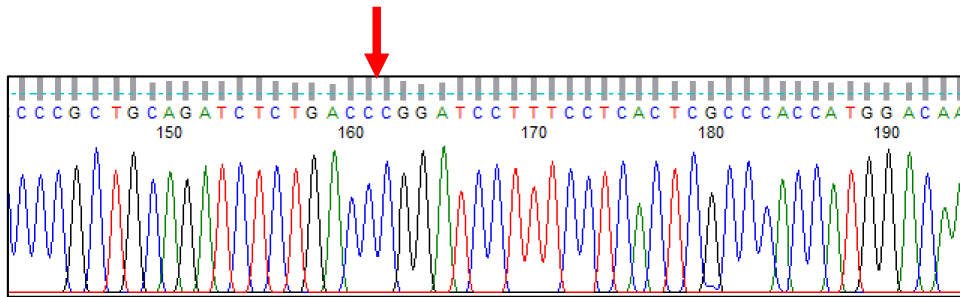


MAAKAEMQLMSPLQISDPFGSFPHAPTMDNYPKLEEMLLSNGAPQFLGAAGAP
EGSGSNSSSSSSGGGGGGGGSNSSSSSSSTFNPQADTGEQPYEHL

FIG. S2C

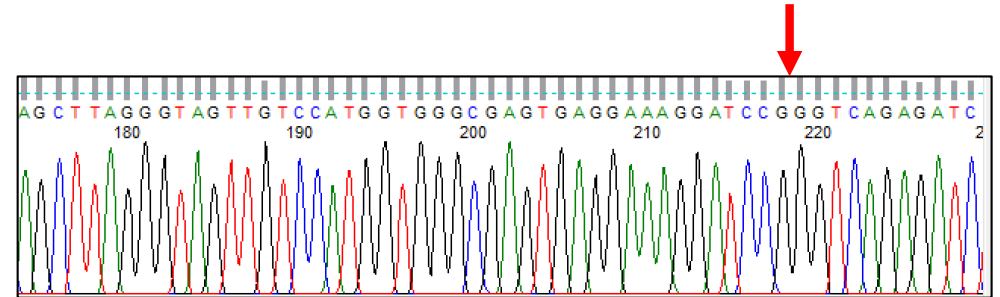
Forward DEL1

Query	92	GCCTGCTCGTCCAGGATGGCCGCGGCCAAGGCCGAGATGCAGCTGATGTCCCCGCTGCAG	151
Sbjct	269	GCCTGCTCGTCCAGGATGGCCGCGGCCAAGGCCGAGATGCAGCTGATGTCCCCGCTGCAG	328
Query	152	ATCTCTGACC---CGGATCCTTTCCTCACTCGCCACCATGGACAACACCCTAAGCTG	207
Sbjct	329	ATCTCTGACC CCGTT CGGATCCTTTCCTCACTCGCCACCATGGACAACACCCTAAGCTG	388
Query	208	GAGGAGATGATGCTGCTGAGCAACGGGGCTCCCCAGTTCCTCGGCGCCGCCGGGGCCCA	267
Sbjct	389	GAGGAGATGATGCTGCTGAGCAACGGGGCTCCCCAGTTCCTCGGCGCCGCCGGGGCCCA	448



Reverse Complement DEL1

Query	134	CAGGATGGCCGCGGCCAAGGCCGAGATGCAGCTGATGTCCCCGCTGCAGATCTCTGACC-	192
Sbjct	280	CAGGATGGCCGCGGCCAAGGCCGAGATGCAGCTGATGTCCCCGCTGCAGATCTCTGACC CC	339
Query	193	---CGGATCCTTTCCTCACTCGCCACCATGGACAACACCCTAAGCTGGAGGAGATGAT	249
Sbjct	340	GTT CGGATCCTTTCCTCACTCGCCACCATGGACAACACCCTAAGCTGGAGGAGATGAT	399
Query	250	GCTGCTGAGCAACGGGGCTCCCCAGTTCCTCGGCGCCGCCGGGGCCCAAGAGGgcagcgg	309
Sbjct	400	GCTGCTGAGCAACGGGGCTCCCCAGTTCCTCGGCGCCGCCGGGGCCCAAGAGGgcagcgg	459

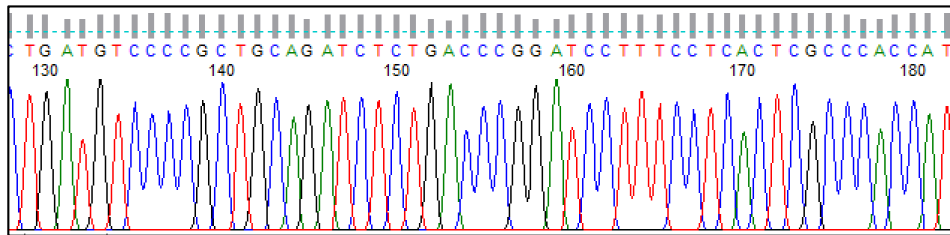


MAAKAEMQLMSPLQISDP**DPFLTRPPWTTTLSWRR***

FIG. S3A

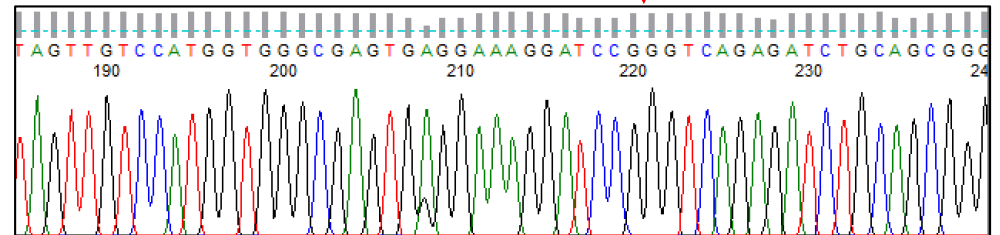
Forward DEL2

Query	78	GCTCTCCAGCCTGCTCGTCCAGGATGGCCGCGGCCAAGGCCGAGATGCAGCTGATGTCCC	137
Sbjct	261	GCTCTCCAGCCTGCTCGTCCAGGATGGCCGCGGCCAAGGCCGAGATGCAGCTGATGTCCC	320
Query	138	CGCTGCAGATCTCTGACC-----GGATCCTTTCTCACTCGCCACCATGGACAAC TACC	193
Sbjct	321	CGCTGCAGATCTCTGACCCTGGTGGATCCTTTCTCACTCGCCACCATGGACAAC TACC	380
Query	194	CTAAGCTGGAGGAGATGATGCTGCTGAGCAACGGGGCTCCCCAGTTCCTCGGCGCCGCCG	253
Sbjct	381	CTAAGCTGGAGGAGATGATGCTGCTGAGCAACGGGGCTCCCCAGTTCCTCGGCGCCGCCG	440



Reverse Complement DEL2

Query	132	CAGGATGGCCGCGGCCAAGGCCGAGATGCAGCTGATGTCCCCGCTGCAGATCTCTGACC-	190
Sbjct	280	CAGGATGGCCGCGGCCAAGGCCGAGATGCAGCTGATGTCCCCGCTGCAGATCTCTGACC	339
Query	191	---GGATCCTTTCTCACTCGCCACCATGGACAAC TACCC TAAGCTGGAGGAGATGAT	247
Sbjct	340	GTTGGATCCTTTCTCACTCGCCACCATGGACAAC TACCC TAAGCTGGAGGAGATGAT	399
Query	248	GCTGCTGAGCAACGGGGCTCCCCAGTTCCTCGGCGCCGCCGGGGCCCCAGAGGGcagcgg	307
Sbjct	400	GCTGCTGAGCAACGGGGCTCCCCAGTTCCTCGGCGCCGCCGGGGCCCCAGAGGGCAGCGG	459



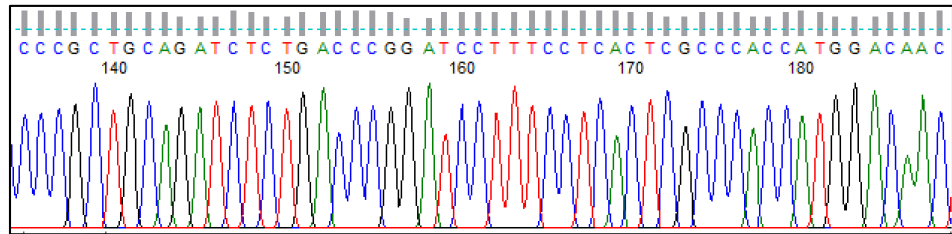
MAAKAEMQLMSPLQISDP**DPFLTRPPWTTTLSWRR***

FIG. S3B

Forward DEL3

```

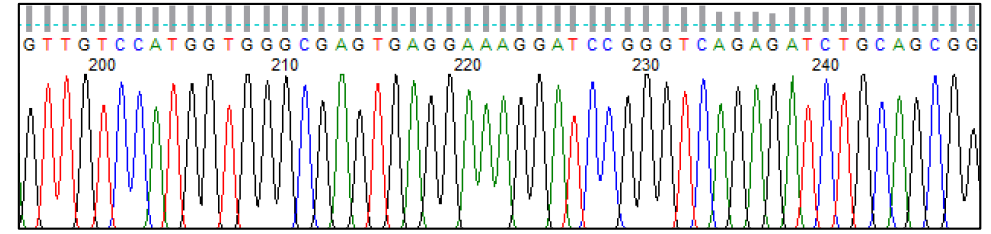
Query 77  GCTCTCCAGCCTGCTCGTCCAGGATGGCCGCGGCCAAGGCCGAGATGCAGCTGATGTCCC 136
Sbjct 261  GCTCTCCAGCCTGCTCGTCCAGGATGGCCGCGGCCAAGGCCGAGATGCAGCTGATGTCCC 320
Query 137  CGCTGCAGATCTCTGACC---CGGATCCTTTCTCACTCGCCACCATGGACAACCTACC 192
Sbjct 321  CGCTGCAGATCTCTGACCCTTGGATCCTTTCTCACTCGCCACCATGGACAACCTACC 380
Query 193  CTAAGCTGGAGGAGATGATGCTGCTGAGCAACGGGGCTCCCCAGTTCTCGGCGCCGCGCG 252
Sbjct 381  CTAAGCTGGAGGAGATGATGCTGCTGAGCAACGGGGCTCCCCAGTTCTCGGCGCCGCGCG 440
  
```



Reverse Complement DEL3

```

Query 132  CAGGATGGCCGCGGCCAAGGCCGAGATGCAGCTGATGTCCCCGCTGCAGATCTCTGACC- 190
Sbjct 280  CAGGATGGCCGCGGCCAAGGCCGAGATGCAGCTGATGTCCCCGCTGCAGATCTCTGACC 339
Query 191  ---CGGATCCTTTCTCACTCGCCACCATGGACAACCTAACCTAAGCTGGAGGAGATGAT 247
Sbjct 340  GTTCGGATCCTTTCTCACTCGCCACCATGGACAACCTAACCTAAGCTGGAGGAGATGAT 399
Query 248  GCTGCTGAGCAACGGGGCTCCCCAGTTCTCGGCGCCGCGGGGCCCCAGAGggcagcgg 307
Sbjct 400  GCTGCTGAGCAACGGGGCTCCCCAGTTCTCGGCGCCGCGGGGCCCCAGAGGGCAGCGG 459
  
```



MAAKAEMQLMSPLQISDP**DPFLTRPPWTTTLSWRR***

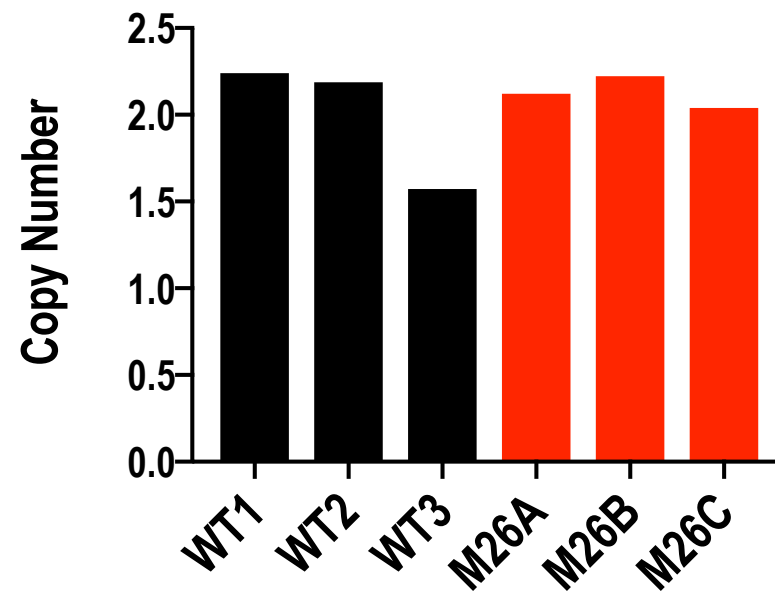


FIG. S4

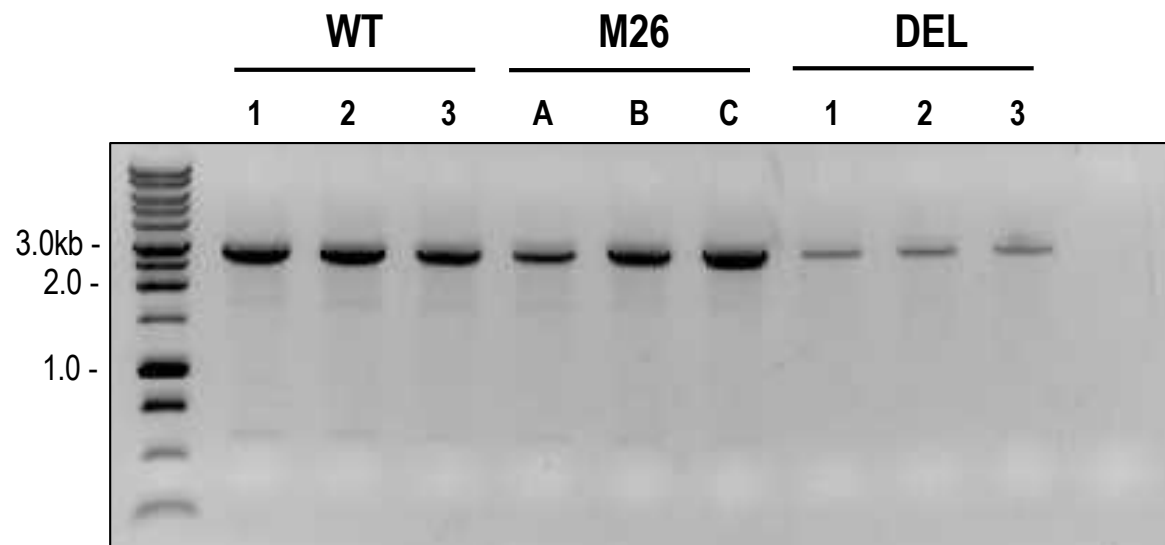


FIG. S5